



RESEARCH ARTICLE

# RNAi-mediated suppression of vimentin or glial fibrillary acidic protein prevents the establishment of Müller glial cell hypertrophy in progressive retinal degeneration

Claire Hippert<sup>1</sup> | Anna B. Graca<sup>1</sup> | Mark Basche<sup>1,2</sup> | Aikaterini A. Kalargyrou<sup>1,2</sup> |  
 Anastasios Georgiadis<sup>1</sup> | Joana Ribeiro<sup>1</sup>  | Ayako Matsuyama<sup>1</sup> | Nozie Aghaizu<sup>1</sup> |  
 James W. Bainbridge<sup>1</sup> | Alexander J. Smith<sup>1,2</sup> | Robin R. Ali<sup>1,2</sup> |  
 Rachael A. Pearson<sup>1,2</sup> 

<sup>1</sup>University College London Institute of Ophthalmology, London, UK

<sup>2</sup>Centre for Cell and Gene Therapy, King's College London, Guy's Hospital, London, UK

## Correspondence

Rachael A. Pearson, Centre for Cell and Gene Therapy, King's College London, 8th Floor Tower Wing, Guy's Hospital, London SE1 9RT, UK.  
 Email: rachael.pearson@kcl.ac.uk

## Present address

Claire Hippert, Hoffman la Roche, Grenzacherstrasse 124, Basel, Switzerland

## Funding information

Fight for Sight UK, Grant/Award Numbers: 1448/1449, 1566/1567; Medical Research Council UK, Grant/Award Numbers: MR/J004553/1, MR/T002735/1; Moorfields Eye Charity, Grant/Award Numbers: E170004A, R150032A, R180005A; Retina UK, Grant/Award Number: GR566; Royal Society, Grant/Award Numbers: RG080398, UF120046

## Abstract

Gliosis is a complex process comprising upregulation of intermediate filament (IF) proteins, particularly glial fibrillary acidic protein (GFAP) and vimentin, changes in glial cell morphology (hypertrophy) and increased deposition of inhibitory extracellular matrix molecules. Gliosis is common to numerous pathologies and can have deleterious effects on tissue function and regeneration. The role of IFs in gliosis is controversial, but a key hypothesized function is the stabilization of glial cell hypertrophy. Here, we developed RNAi approaches to examine the role of GFAP and vimentin in vivo in a murine model of inherited retinal degeneration, the *Rhodopsin* knockout (*Rho*<sup>-/-</sup>) mouse. Specifically, we sought to examine the role of these IFs in the establishment of Müller glial hypertrophy during progressive degeneration, as opposed to (more commonly assessed) acute injury. Prevention of *Gfap* upregulation had a significant effect on the morphology of reactive Müller glia cells in vivo and, more strikingly, the reduction of *Vimentin* expression almost completely prevented these cells from undergoing degeneration-associated hypertrophy. Moreover, and in contrast to studies in knockout mice, simultaneous suppression of both GFAP and vimentin expression led to severe changes in the cytoarchitecture of the retina, in both diseased and wild-type eyes. These data demonstrate a crucial role for Vimentin, as well as GFAP, in the establishment of glial hypertrophy and support the further exploration of RNAi-mediated knockdown of vimentin as a potential therapeutic approach for modulating scar formation in the degenerating retina.

## KEYWORDS

degeneration, GFAP, glial scar, gliosis, hypertrophy, intermediate filament, Müller cells, retina, vimentin

Claire Hippert and Anna B. Graca are joint-first authors.

This is an open access article under the terms of the Creative Commons Attribution License, which permits use, distribution and reproduction in any medium, provided the original work is properly cited.

© 2021 The Authors. GLIA published by Wiley Periodicals LLC.

## 1 | INTRODUCTION

Reactive gliosis is regarded as a cellular attempt to protect the surrounding tissue from further damage, in order to promote repair and limit neuronal re-modeling. It includes morphological, biochemical, and physiological changes, each of which can vary with the type and severity of the initiating insult (Silver & Miller, 2004). In the eye, gliosis involves primarily Müller glial cells, which span the retina and provide structural and metabolic support to the surrounding neurons. In lower vertebrates, Müller cells may attempt to repair the damaged retina by de-differentiating into progenitor-like cells in response to injury (Jadhav, Roesch, & Cepko, 2009) but this capacity is largely lacking in the mammalian retina (Löffler, Schafer, Volkner, Holdt, & Karl, 2015). Instead, reactive gliosis is characterized by the upregulation of intermediate filament proteins (IFs), particularly glial fibrillary acidic protein (GFAP) and vimentin, and glial hypertrophy, which involves the extension, thickening and stabilization of glial processes. Depending on the injury, some of these processes can extend beyond the outer limiting membrane (OLM) into the subretinal space between the neural retina and the retinal pigment epithelium (RPE; Hippert et al., 2015; Lewis & Fisher, 2000; Pearson et al., 2010; Winkler, Hagelstein, Rohde, & Laqua, 2002). In addition, there is a concomitant increase in the deposition of inhibitory extracellular matrix (ECM) molecules, such as chondroitin sulfate proteoglycans (CSPGs; Chen, FitzGibbon, He, & Yin, 2012; Hippert et al., 2015). Together, these lead to the formation of an inhibitory “scar” at the apical edge of the neural retina (Bringmann et al., 2006).

Müller glial cell reactive gliosis has been reported as a response to various retinal pathologies, including inherited retinal degeneration (Hippert et al., 2015), and geographic atrophy and wet age-related macular degeneration (Wu, Madigan, Billson, & Penfold, 2003). Prolonged gliosis, as can occur with chronic degeneration, can have deleterious effects on tissue function and is considered to be a major factor limiting endogenous regeneration throughout the central nervous system (CNS; Bringmann et al., 2006; Burns & Stevens, 2018; Fawcett & Curt, 2009). The glial scar may impede neuronal cell migration and axonal regrowth either by presenting a physical barrier in the form of hypertrophic glial processes, or a reservoir of inhibitory ECM molecules, or a combination of these (Chan, Wong, Liu, Steeves, & Tetzlaff, 2007; Cregg et al., 2014). In the eye, it has been postulated that it may prevent Müller glial cell-cycle re-entry, while the expansion of hypertrophic Müller glial processes into the subretinal space forms fibrotic tissue that has been shown to block the regeneration of outer segments and exacerbates retinal detachment (Lewis & Fisher, 2000). Gliosis is also understood to impede the efficacy of many proposed therapeutic approaches, including viral vector transduction in ocular gene therapy (Calame et al., 2011) and the ability of retinal grafts, cell transplants and electronic implants to interact with the overlying host retina (Barber et al., 2013; Hippert et al., 2015; Pearson, Hippert, Graca, & Barber, 2014; Tassoni, Gutteridge, Barber, Osborne, & Martin, 2015).

Identifying precisely which aspects of reactive gliosis impede therapeutic interventions in vivo and finding ways to ameliorate them

is challenging but crucial (Burns & Stevens, 2018; Hamby & Sofroniew, 2010). Recent evidence has suggested that the stiffness of the glial scar affects the regenerative properties of nervous tissue and that changes in IF expression levels correlates with changes in cell stiffness (Lu et al., 2011; Moeendarbary et al., 2017; L. Wang et al., 2018). An increase in GFAP is considered the hallmark of reactive gliosis and GFAP is thought to be critically important in the formation of the extended and thickened (hypertrophic) astrocytic processes typically seen in reactive gliosis (Lundkvist et al., 2004; Pekny, Wilhelmsson, & Pekna, 2014). Conversely, vimentin has received much less attention, perhaps because of the less dramatic changes in its expression upon injury.

Here, we use RNAi to modulate the expression of *Gfap* or *Vimentin* in a mouse model of inherited, progressive retinal degeneration. We report a crucial role for vimentin, as well as GFAP, in the establishment of retinal glial hypertrophy. This also raises the potential utility of RNAi-mediated knockdown of vimentin as a therapeutic approach for modulating glial hypertrophy as part of scar formation in the damaged retina.

## 2 | MATERIALS AND METHODS

### 2.1 | Animals

*Rlbp.Gfp*<sup>+/+</sup> (E. Levine, University of Utah; Vazquez-Chona, Clark, & Levine, 2009), *Rho*<sup>-/-</sup> (P. Humphries, Trinity College Dublin) and C57Bl/6J wild-type (Harlan, UK) mice were housed in University College London facilities and kept on a standard 12:12 light: dark cycle. Mice received food and water *ad lib.* and were provided with fresh bedding and nesting. *Rlbp.Gfp*<sup>+/+</sup> mice were used at postnatal (P)7–8. *Rho*<sup>-/-</sup> and wild-type animals were aged P10 (±1 day) at the time of AAV injection, unless otherwise stated. Both male and female animals were used in all experiments. All experiments have been conducted in accordance with the United Kingdom Animals (Scientific Procedure) Act of 1986.

### 2.2 | Plasmid construction

shRNA constructs for *Gfap* and *Vimentin* were generated by subcloning the target hairpins (shGfap or shVim) into the mU6pro plasmid. The target hairpins were placed downstream of a U6 promoter to form an RNAi-expression cassette. The RNAi cassettes were excised and cloned into an AAV pD10.CBA backbone containing a Red Fluorescent Protein (RFP) reporter. The shGfap targets the *Gfap* sequence 5'-GCACGAAGCTAACGACTAT-3' (position nt 911. NM\_010277) and the shVim targets the *Vimentin* sequence 5'-GTGAGATGGAAGAGAATTT-3' (position nt 1,155. NM\_011701). ShGfap and shVim hairpins were designed using a standard shRNA motif of sense-loop-antisense in which the loop consisted of nine nucleotides. shRNA is less likely to generate off-target effects compared to siRNA, but the selected sequences were further verified for

low likelihood of off-target effects by using web-based RNAi design software (Dharmacon, Invitrogen) where genome-scanning algorithms assess the sequences for homology with the rest of the genome; the selected shRNA sequences were found to be highly specific and on-target. Non-targeting hairpin was used as a control (shControl), the sequence used for this was: 5'-GATCGGACACTCCTCATAA-3'. The resulting constructs were named pshGfap, pshVim, and pshControl. The sequences most effective for knocking down *Gfap* (pshGfap2) and *Vimentin* (pshVim4) (See Results) were used to generate a long hairpin (plh) to knockdown *Gfap* and *Vimentin* simultaneously. *Gfap* expression plasmid (pGfap) was generated by using pCR4-Gfap (Source Bioscience, Cambridge, UK) *Vimentin* expression plasmid (pVimentin) was purchased from Origene (MR207446). The RFP sequence in the AAV pD10.CBA/RFP backbone was then replaced by either *Gfap* or *Vimentin*, respectively. All constructs were verified by sequencing (Beckman Coulter Genomics).

### 2.3 | Cell transfection

Human embryonic kidney (HEK) cell line 293 T cells were seeded in 24-well plates at a density of  $1.5 \times 10^5$  cells per well in 1 ml of Dulbecco's modified Eagle's medium (DMEM; Invitrogen [Thermo-Scientific, Loughborough, UK]) supplemented with 10% fetal bovine serum (FBS) and 1% antibiotic/antimycotic solution (AA) and incubated at 37°C/5% CO<sub>2</sub>. Transfections were performed using Lipofectamine 2000 reagent (Invitrogen), per the manufacturer's instructions. The day after seeding, cells were co-transfected with 200 ng or 800 ng of the hairpin RNA constructs and 200 ng of either pGfap or pVimentin or both together. Transfected cells were harvested 48 hr later for quantitative RT-PCR.

### 2.4 | Generation and purification of AAV vectors

PshGfap2, pshVim4 and pshlh were used to produce AAVShH10-Y445F (herein termed AAV-shGfap, AAV-shVim, and AAV-lh, respectively). Recombinant AAVShH10.Y445F<sup>34</sup> vectors were produced through a tripartite transfection as described earlier (Gao et al., 2002) followed by purification using AVB Sepharose high performance affinity medium (GE Healthcare, Hatfield, UK). The virus preparation was concentrated using a Vivaspin 4 concentrator (10 kDa, Sartorius Stedim Biotech, Viral Fisher Scientific, Loughborough, UK), to 60 µl. Viral particle titers, in terms of vg/mL, were determined by quantitative PCR relative to standards. The resulting AAV preparations, AAV-shGfap, AAV-shVim, AAV-lh and AAV-shControl, were always titer matched before use.

### 2.5 | Müller glia primary culture and viral vector transduction

Retinae were dissected from the eyes of P7-8 *Rlbp.Gfp*<sup>+/+</sup> mice and cells were dissociated with a papain-based kit (Worthington

Biochemical, Lorne Laboratories, Reading, UK). Reagents were formulated according to manufacturer's instructions and cells were prepared in a manner similar to that used for the preparation of photoreceptor precursors, as reported previously (Pearson et al., 2012). Briefly, cells were dissociated for 30 min and then gently triturated, passed through a 70-µm cell strainer, and centrifuged at 200g for 5 min. Pellets were resuspended in 10% ovomucoid inhibitor solution (OMI) containing DNase I (100 U/ml) and incubated for 10 min before layering over OMI and centrifuging at 100g for 5 min. The cell pellet was resuspended in EBSS/1% FBS before undergoing FACS sorting. FACS was carried out with Cell Sorter MoFlo XDP (Beckman Coulter, High Wycombe, UK) and green fluorescent protein (GFP) positive cells were collected in EBSS/FBS (1:1) medium. Cells were spun down for 20 min at 250 g, resuspended in DMEM/10% FBS/1% AA medium and then seeded into eight-well imaging chamber plates (PAA, GE Healthcare, Austria) pre-coated with laminin (5 µg/ml, Sigma Aldrich, UK) at a density of 125,000 cells per cm<sup>2</sup> and incubated at 37°C/5% CO<sub>2</sub> for 2–3 weeks. Wells of equivalent confluency were used for further assessment.  $5 \times 10^{12}$  particles of each vector/well were then added to the Müller glia cultures. One week post-transduction cells were harvested either for quantitative RT-PCR or fixed for immunocytochemistry. No marked differences in number of cells/well were observed between conditions after transfection. To determine AAV transduction efficiency cells were FACS-sorted for RFP fluorescence.

### 2.6 | Astrocyte primary culture

Brains of P7-8 pups were dissected per previously established protocols (Schildge, Bohrer, Beck, & Schachtrup, 2013) and put into a petri dish containing cold Hank's Balanced Salt Solution (HBSS, Gibco, Thermo-Scientific, Loughborough, UK). Briefly, the meningeal layer was carefully removed from both hemispheres and the cortices were separated from the rest of the brain manually and placed in a new petri dish containing HBSS. Collected tissue was cut into small pieces using dissection scissors. The harvested tissue was transferred into a 15 mL sterile falcon tube and centrifuged at 200g for 5 min. The supernatant was aspirated, and cortices were resuspended in 1 ml/per brain of 0.05% trypsin/DNase and incubated at 37°C/5% CO<sub>2</sub> for 20 min. After incubation, the cell suspension was passed through a 40 µm cell strainer and centrifuged for 10 min at 200g. Trypsin solution was removed, and cell pellet was gently washed with PBS before being resuspended in DMEM/10% FBS/1% AA medium and seeded into six-well poly-D-lysine coated plates (Invitrogen). After 2 weeks in culture, astrocytes were transfected with  $5 \times 10^{12}$  particles of AAV-shControl vector and fixed for immunocytochemistry 1 week post-transduction.

### 2.7 | Intravitreal injection of viral vectors

P10 or 4.5 week old *Rho*<sup>-/-</sup> mice were anesthetized with an intraperitoneal injection of a mixture of Dormitor (1 mg/ml medetomidine hydrochloride; Pfizer Pharmaceuticals, Walton Oaks, UK), ketamine

(100 mg/ml; Fort Dodge Animal Health, Sandwich, UK), and sterile water in the ratio 5:3:42. Surgery was performed under direct visual control using an operating microscope. A sterile 34 gauge hypodermic needle (Hamilton, Fischer-Scientific, Loughborough, UK) was passed through the sclera, at the superior equator and next to the limbus, into the vitreous cavity. Injection of 1  $\mu$ l virus containing  $5 \times 10^{12}$  virus particles was made with direct observation of the needle in the center posterior region of the vitreous cavity. Note that for co-administration of AAV-shGfap and AAV-shVim, 1  $\mu$ l of each virus, each containing  $5 \times 10^{12}$  virus particles, was administered per eye. Control eyes received 2  $\mu$ l containing a total of  $1 \times 10^{13}$  virus particles of AAV-shControl, to provide a volume and titer-matched control. Eyes were harvested at either 3 or 6 weeks post-injection for quantitative RT-PCR or fixed and embedded for immunohistochemistry.

## 2.8 | Quantitative RT-PCR

RNA was extracted from cultured cells or dissociated neural retinae using RNeasy Mini or Micro Kit (Qiagen, West Sussex, UK) and cDNA preparation was performed using QuantiTect Reverse Transcription Kit or whole transcriptome Kit (Qiagen) per the manufacturer's instructions. Relative quantification by RT-PCR of *Gfap* or *Vimentin* against endogenous  $\beta$ -actin expression levels were measured using primers and probes included in Table S1.

## 2.9 | Histology, immunohistochemistry, and immunocytochemistry

Müller glia cell cultures were fixed for 1 hr in 4% paraformaldehyde (PFA). Eyes were fixed in 1% (for immunohistochemistry) PFA for 1 hr before embedding in OCT (RA Lamb, Eastbourne, UK) and freezing in isopentane precooled in liquid nitrogen. Cryosections were cut at 18  $\mu$ m and all sections were collected for analysis. Cryosections were air-dried for 30 min and washed in phosphate-buffered saline (PBS). Sections and fixed Müller glia cell cultures were pre-blocked for 1 hr at room temperature (RT) in a blocking solution: 2% normal goat serum (NGS; Ab Serotec, Oxford, UK), 1% bovine serum albumin (BSA; Sigma Aldrich, Dorset UK), 0.5% triton-X in PBS. They were then incubated for 2 hr at RT with the appropriate primary antibody. After rinsing with PBS, they were incubated for 1 hr at RT with secondary antibody, goat anti-rabbit, anti-chicken or anti-mouse 488 (Molecular Probes, Thermo-Scientific, Loughborough, UK) as appropriate. They were rinsed and counter-stained with Hoechst 33342 for 5 min before mounting. Negative controls omitted the primary antibody.

Primary antibodies included: polyclonal rabbit anti-GFAP (DAKO; #Z0334); monoclonal mouse anti-vimentin (Sigma-Aldrich [Gillingham, Dorset, UK]; #099K4753; for histochemistry); polyclonal chicken anti-vimentin (Millipore [Watford, UK]; AB5733; for cytochemistry), monoclonal mouse anti-CRALBP (Abcam [Watford, UK]; #ab15051), purified anti-Glutamine Synthetase (BD Transduction Laboratories

[Wokingham, UK]; #610517), polyclonal rabbit anti-SOX9 (Millipore; #AB5535) and monoclonal mouse anti-CS-56 (Sigma; #C8035).

Retinal flat mounts were prepared by excising the eye, as before, and carefully removing the sclera and retinal pigmented epithelium (RPE). The neural retina was fixed in 4% PFA for 1 h and counter-stained with Hoechst 33342 before being cut to create four conjoined "petals" (from the periphery towards the optic nerve), which were then flattened out on a slide. A drop of fluorescent mounting medium (DAKO, Ely, UK) was placed upon the tissue and the coverslip was then carefully placed on top of it.

## 2.10 | Confocal microscopy

Retinal sections and Müller glial cell cultures were viewed on a confocal microscope (Leica TCS SPE, Leica Microsystems, Milton Keynes, UK). Retinal images show merged projection images of an xyz confocal stack through retinal sections, approximately 18  $\mu$ m thick, as stated. Müller glia images show xyz confocal stacks through the depth of the culture (approximately 5–10  $\mu$ m). Individual z images were acquired using a 2-frame average and at 1,024 x 1,024 resolution and at approximately 1  $\mu$ m step intervals throughout the depth of the stack. The same laser intensity, gain and offset settings were used when comparing expression of GFAP or vimentin between the different conditions. Retinal flat mounts were imaged as above but taking an xyz stack through the entire thickness of the retina (150–200  $\mu$ m) at 0.5  $\mu$ m z-steps.

## 2.11 | Müller cell 3D reconstruction

Leica confocal xyz images (in tiff format) were directly opened in Amira 5.5.0 (FEI.com). Data series were filtered using a noise reduction median filter and then individual cells were semi-automatically segmented using a Wacom drawing tablet. The segmentation data was smoothed and "islands" with connected area of voxels containing a number of voxels less than or equal to the size value specified were removed. Three-dimensional surfaces were generated and shown using vertex normals. Three to five cells were reconstructed per file. All data were treated in the same way.

## 2.12 | Müller cell apical process measurement

The area occupied by the apical terminal processes of transduced Müller glia was measured using Image J (Open Source; [imagej.nih.gov/ij/](http://imagej.nih.gov/ij/)) and GNU Image Manipulation Programme (GIMP; Open Source; <https://www.gimp.org/>). Orthogonal views of the individual sub-stacks were used to track individual cells to their end-foot processes. Only those end-feet that could be clearly identified as being associated with cell bodies that occupied a position in the inner nuclear layer (INL) were used for assessment. Sub-stack xy projections encompassing the first 15–20  $\mu$ m at the apical margin of the retina



were generated from the flatmount confocal xyz stacks described above. The resulting image was then opened using GIMP software and converted to grayscale. Threshold Alpha tool was used to

separate signal from background and the same threshold was applied to all analyzed images. Regions of interest (ROI) were selected using the free selection tool. The perimeter of each individual end-foot

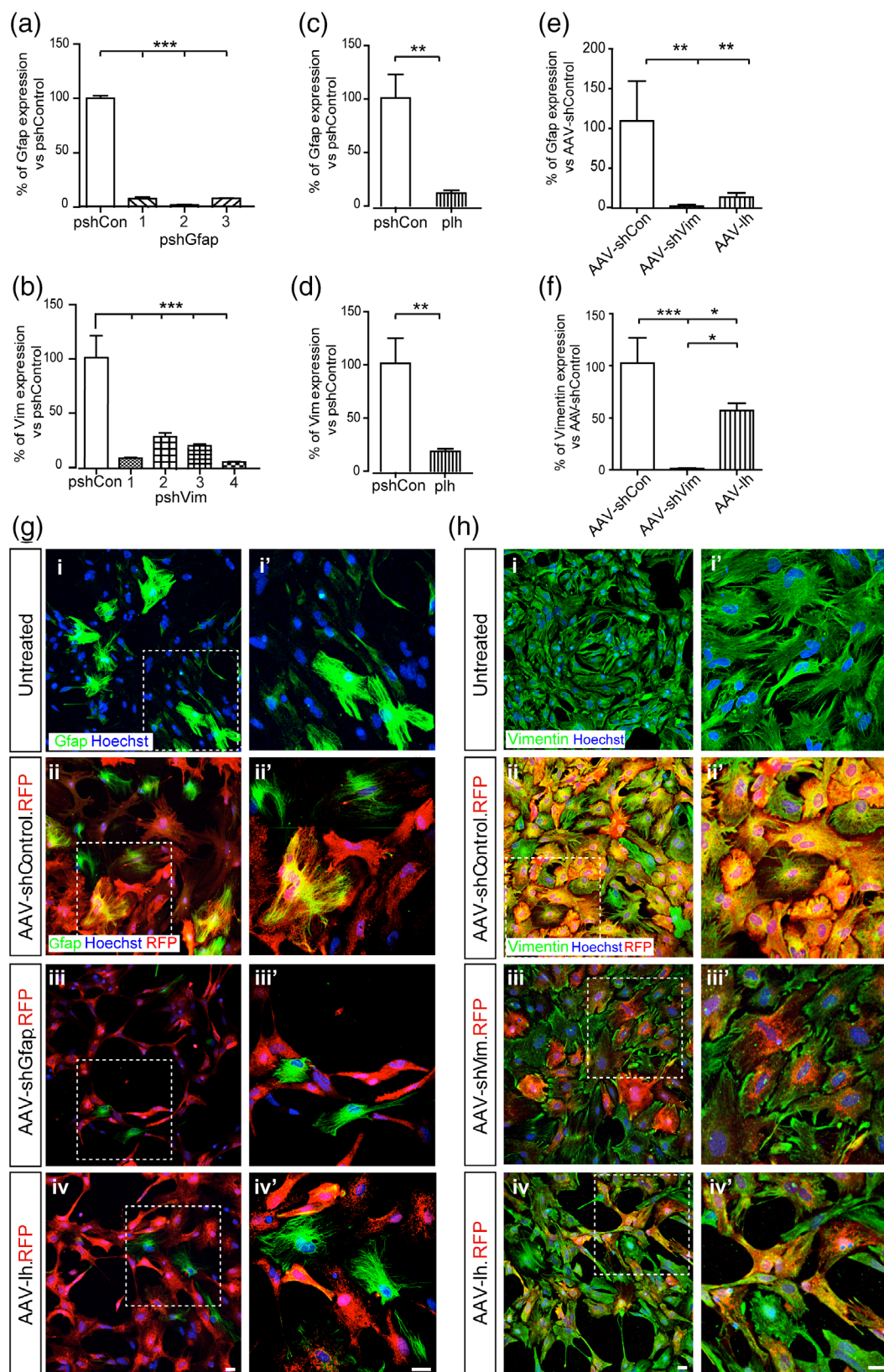


**FIGURE 1** Legend on next page.

process was manually delineated and the histogram dialogue was used to quantify the total number of pixels within the selected area. The measured values for the total area were then converted to  $\mu\text{m}^2$ . All quantifications were made by an independent assessor in a fully blinded manner. These values are presented in the text and were used for statistical analysis. A second assessor analyzed the same data sets for verification purposes. The two assessors made independent selections of end-feet to measure. These data are presented in Supplementary Information (see Figure S5).

## 2.13 | Statistics

All means are reported as means  $\pm$  SD unless otherwise stated.  $n$  = number of independent retinæ or cultures, where appropriate. qRT-PCR results are based on at least two independent Müller cell primary cultures or cohorts of animals, as appropriate. All in vivo assessments are based on  $N > 3$  independent retinæ per condition. Statistical significance was assessed using the Graphpad Prism 5 software and denoted as  $p < .05 = *$ ,  $p < .01 = **$ ,  $p < .001 = ***$ . As not all data were normally distributed, as assessed using the d'Agostino and Pearson omnibus normality test, nonparametric  $t$ -tests and one-way ANOVAs were applied as specified in the figure legends. Corrections for multiple comparisons were applied, where necessary.

## 3 | RESULTS

### 3.1 | AAV-shGfap and AAV-shVim mediate effective knockdown of endogenous Gfap and Vimentin in Müller cell primary cultures

Despite intense investigation, the roles of GFAP and other IFs in gliosis, particularly hypertrophy, remain unclear. This is in part due to a reliance on knockout models, in which the protein in question is absent from the point of conception onwards, leading to the possibility of compensatory upregulation in other related proteins. The use of knockout models has also necessitated the use of acute injury models. Here, we sought to explore the role of GFAP and vimentin in prolonged gliosis, as occurs in progressive retinal degeneration. We therefore designed RNA interference (RNAi) strategy that could be introduced into models of inherited

retinal degeneration at different time points, both before and after the establishment of Müller Glial hypertrophy.

*Gfap* and *Vimentin* silencing hairpins and non-targeting control (shControl) were designed (Table S2) and verified in vitro (Figure 1a, b). The most effective (shGfap2 and shVim4) were selected to generate a long hairpin (lh) for the simultaneous silencing of both *Gfap* and *Vimentin* mRNA (Figure 1c,d). The relevant constructs were packaged into adeno-associated viral (AAV)-ShH10-Y445F. This vector is reported to preferentially targets Müller glial cells following intravitreal injection in rats, although some ganglion cell labeling was also evident (Klimczak, Koerber, Dalkara, Flannery, & Schaffer, 2009). In our hands, labeling was largely restricted to Müller glia and retinal ganglion cells in the mouse retina (Figure S1a).

AAV-shGfap, AAV-shVim and AAV-lh (long hairpin) were assessed for their ability to silence endogenous expression of *Gfap* and *Vimentin* in cultured primary Müller glial cells in vitro. *Rbpl1.Gfp*<sup>+/+</sup> postnatal day (P)7–8 Müller glial cells were isolated by FACS and cultured for 2–3 weeks, retaining a broad spectrum of Müller glia markers (Figure S1b). RFP was detectable within 2 days, and in more than 97% of cells 1-week post-transduction with AAV-shControl, AAV-shGfap or AAV-shVim (– Figure S1c–e). Qualitatively, transduction resulted in some morphological changes, at least for those treated with AAV-shGfap, which became thinner and developed a more elongated profile (Figure 1g,h; Figure S1c).

Expression levels of *Gfap* and *Vimentin* were assessed 1-week post-transduction, using qRT-PCR and immunocytochemistry (ICC) analysis (Figure 1e–h). Endogenous GFAP protein levels were variable both between and within individual Müller cell primary cultures (Figure 1gi). Nonetheless, *Gfap* RNA levels were significantly reduced by AAV-shGfap and by AAV-lh, to 2.4% ( $\pm 1.9$ ) and 13.6% ( $\pm 5.4$ ) of AAV-shControl levels, respectively ( $n = 3$  independent cultures; Figure 1e). This was confirmed by ICC, with little or no GFAP detectable in RFP+ cells receiving AAV-shGfap (Figure 1giii). GFAP levels were similarly reduced in cells transduced with AAV-lh (Figure 1giv).

*Vimentin* was robustly expressed in most cells in Müller cell primary cultures (Figure 1hi). *Vimentin* RNA levels were significantly reduced by 1-week post-transduction with AAV-shVim, to 1.4% ( $\pm 0.4$ ) of AAV-shControl levels ( $n = 3$  for each condition; Figure 1f). Application of AAV-lh also led to a statistically significant but much smaller reduction in *Vimentin* RNA; 57.1% ( $\pm 6.8$ ) of the AAV-shControl levels. ICC confirmed a robust reduction in vimentin staining in AAV-shVim transduced cells (Figure 1hiii) compared to controls. Vimentin was

**FIGURE 1** RNAi targeting vectors mediate robust knockdown of *Gfap* and *Vimentin* in cultured Müller glia in vitro (a–d), histograms show knockdown of *Gfap* and *Vimentin* RNA, as assessed by qRT-PCR at 48 hr post-transfection, in HEK-293T cells following co-transfection of (a) pshGfap, (b) pshVim or (c, d) plh (long hairpin) constructs with pGfap or pVimentin (or both for c, d), respectively (1:1 ratio).  $**p < .01$  and  $***p < .001$  with a one-way ANOVA with Bartlett's corrections for pshGfap and pshVim;  $t$ -test for lh. Error bars: SD  $n = 3$  independent cultures per group. (e, f) Histogram shows RNA levels, assessed by RT-qPCR 1 week post-transduction, for (e) *Gfap* and (f) *Vimentin* following transduction of Müller glial cultures with AAV-shGfap, AAV-shVim or AAV-lh, respectively. (g) Immunocytochemistry shows that GFAP expression (green) is highly variable between cells both in (i) untreated and (ii) AAV-shControl treated (red) cultures. However, GFAP was reduced in cells transduced with (iii) AAV-shGfap (red) or (iv) AAV-lh (red), compared to controls. (h) Immunocytochemistry shows robust expression of vimentin (green) in most (i) untreated and (ii) AAV-shControl-treated (red) cells. Expression was markedly reduced in cells transduced with (iii) AAV-shVim (red) or (iv) AAV-lh (red), compared to controls. Cells were counterstained with nuclei marker Hoechst 33342 (blue). (i'–iv') show ROIs outlined in (i–iv).  $*p < .05$ ,  $**p < .01$  and  $***p < .001$  with a one-way ANOVA with Tukey's for multiple comparisons. Error bars: SD  $n \geq 3$  independent cultures per group. Scale bar: 25  $\mu\text{m}$  [Color figure can be viewed at [wileyonlinelibrary.com](http://wileyonlinelibrary.com)]

reduced in AAV-Ih transduced cells, although in keeping with the qRT-PCR analysis, a number of RFP<sup>+</sup> cells retained some expression of vimentin (Figure 1hiv).

### 3.2 | AAV-shGfap and AAV-shVim mediate effective knockdown of endogenous *Gfap* and *Vimentin* in vivo in *Rho*<sup>-/-</sup> mice

We next assessed AAV-shGfap and AAV-shVim in vivo. We chose the *Rho*<sup>-/-</sup> model of inherited retinal degeneration because it exhibits a moderate rate of photoreceptors loss (compared to very

fast models like *PDEβ*<sup>(rd1/rd1)</sup> and much slower models like *Prph2*<sup>(rd2/rd2)</sup>) and we have previously found it to exhibit a strong upregulation of *Gfap* and vimentin and clear evidence of Müller glia hypertrophy (Hippert et al., 2015; Pearson et al., 2010). In the first instance, vector was administered at P10 since Müller glia become post-mitotic in the central retina by P6 (Jadhav et al., 2009) and retinogenesis is complete by P10 in the rodent retina (Young, 1985). Degeneration and the concomitant reactive gliosis begins shortly after this in the *Rho*<sup>-/-</sup> mouse (Hippert et al., 2015; Humphries et al., 1997). Recipient P10 *Rho*<sup>-/-</sup> mice received AAV-shControl, AAV-shGfap or AAV-shVim intravitreally and were assessed 3 weeks later in the first instance.

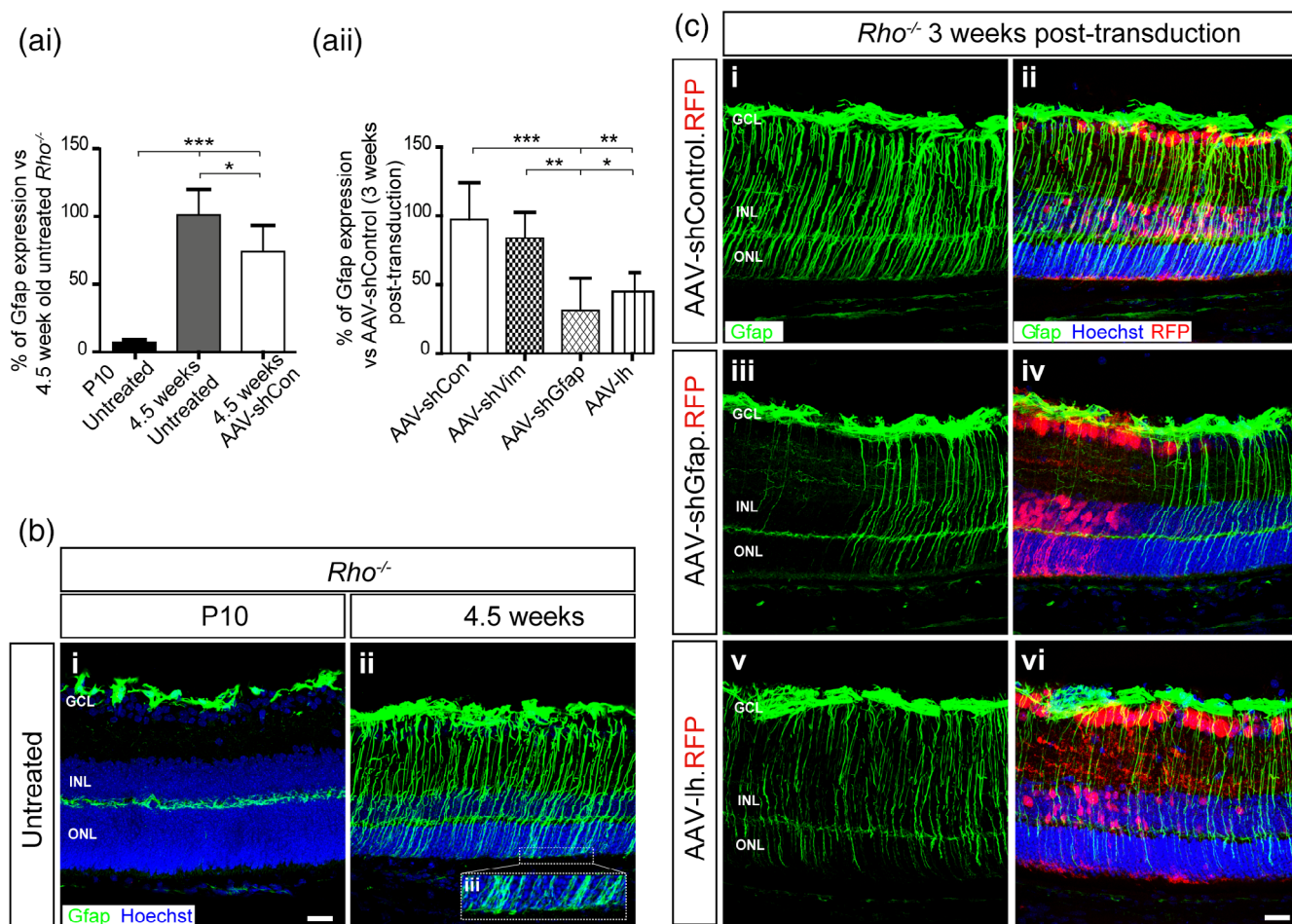


**FIGURE 2** RNAi targeting vectors mediate knockdown of GFAP in Müller glia in vivo in the degenerating retina. (ai) Histogram shows that *Gfap* mRNA levels, as assessed by RT-qPCR, are low at the time of injection (P10) but increase significantly during degeneration. Administration of AAV-shControl vector led to a small but significant reduction in *Gfap* mRNA. (ii) Administration of either AAV-shGfap or AAV-Ih mediated significant reductions in *Gfap* mRNA, compared to AAV-shControl, while no off-target effects were seen with AAV-shVim.  $p < .05 = *$ ,  $p < .01 = **$ ,  $p < .001 = ***$  with a one-way ANOVA. Error bars: SD  $n \geq 5$  independent retinæ per group. (b) Immunohistochemistry shows that in the (i) P10 *Rho*<sup>-/-</sup> retina, GFAP expression (green) is largely restricted to astrocytes at the vitreal surface of the GCL, with some additional expression around the outer plexiform layer (OPL). (ii) By 4.5 weeks of age, in *Rho*<sup>-/-</sup> retina, GFAP is expressed by the majority of Müller glia cells and throughout the entire length of their processes. (iii) Close inspection of the outer retina reveals the extension of apical Müller glia GFAP<sup>+</sup> processes along the outer edge of the ONL, which led to development of a "glial scar." (ci,ii) GFAP expression was unchanged at 3 weeks post-injection (4.5 weeks of age) following transduction with AAV-shControl vector. (iii,iv) In those eyes receiving AAV-shGfap, GFAP expression was largely absent in transduced cells (red) and only seen in non-transduced cells. (v,vi) GFAP expression was also reduced in cells transduced with AAV-Ih, albeit to a lesser extent. Retinal cryosections were counterstained with nuclei marker Hoechst 33342 (blue). GCL, ganglion cell layer; INL, inner nuclear layer; ONL, outer nuclear layer. Scale bar: 25  $\mu$ m [Color figure can be viewed at [wileyonlinelibrary.com](http://wileyonlinelibrary.com)]



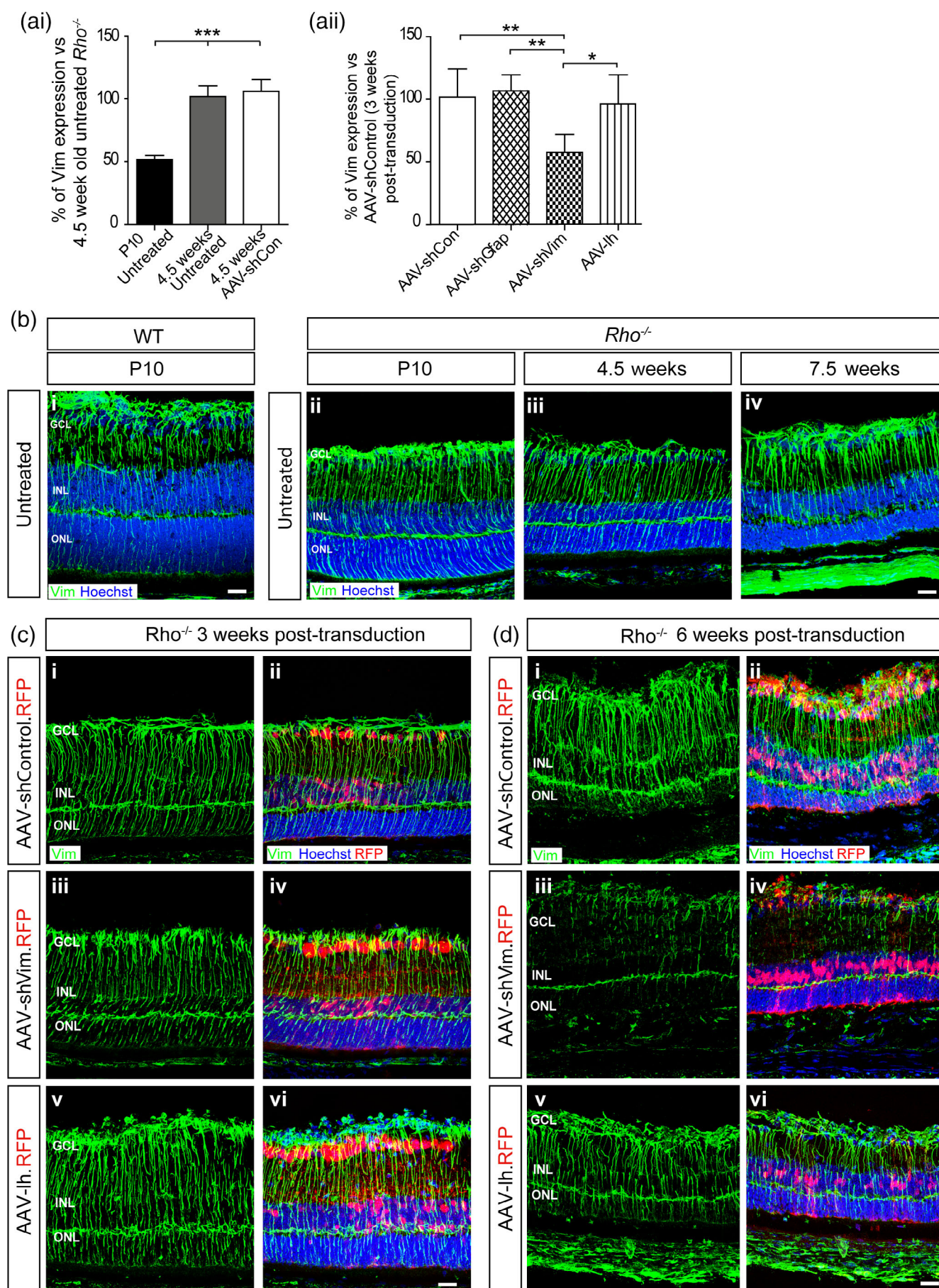


**FIGURE 3** Legend on next page.

In the untreated *Rho*<sup>-/-</sup> mouse (Figure 2ai, bi), *Gfap* expression is very low at P10 and largely restricted to the outer edge of the ganglion cell layer (GCL) and the outer plexiform layer (OPL; Figure 2ai). It is markedly upregulated during the course of degeneration and by 4.5 weeks of age, GFAP is widespread and demarcates the full extent of the Müller glial processes, which appear thickened (Figure 2bii). Close inspection of the apical margin of the neural retina reveals the lateral extension of terminal GFAP<sup>+</sup> processes along the outer edge of the outer nuclear layer (ONL; Figure 2biii).

Administration of AAV-shControl led to a small, but statistically significant, reduction in *Gfap* mRNA (Figure 2ai) compared to un-injected controls, although this did not result in a noticeable reduction in GFAP as assessed by IHC (Figure 2ci,ii). However, given this result, and because the assessment of Müller Glial morphology (see later) necessitates the use of the RFP reporter within both control and RNAi-containing vectors, the effects of AAV-shGfap and AAV-shVim were compared against AAV-shControl, as opposed to untreated controls. As such, any effect seen compared to shControls is likely to represent a modest underestimate of the effect compared with untreated controls. AAV-shGfap significantly reduced total *Gfap* RNA levels, to 31.5% ( $\pm 23.2$ ) of AAV-shControl levels, while GFAP protein levels were negligible in Müller glia transduced with AAV-shGfap (Figure 2ciii,iv), compared to those transduced with AAV-shControl (Figure 2ci,ii). While these vectors effectively transduce astrocytes in vitro (see Klimczak et al., 2009 and Figure S2a), transduction of astrocytes in vivo was extremely low and GFAP levels remained robust (Figure S2b and Figure 2ciii,vi). Moreover, transduction spread does not always encompass the whole retina (see Figure 2civ). Together, these likely explain the more modest reduction in *Gfap* mRNA in vivo, compared to in vitro assessments of purified Müller glia. Of note, AAV-shVim had no indirect or compensatory effect on the expression of *Gfap* (Figure 2aii). The expression of other IFs (e.g., nestin, synemin) was not assessed in this study.

In the untreated P10 *Rho*<sup>-/-</sup> mouse, *Vimentin* is expressed throughout the retina (Figure 3ai,bii-iv and Hippert et al., 2015). Administration of AAV-shControl had no indirect effect on *Vimentin* RNA levels, compared to untreated retinæ (Figure 3ai), but for consistency all data is presented normalized against shControl levels. At 3 weeks post-transduction, AAV-shVim significantly reduced *Vimentin* RNA levels, to 57.5% ( $\pm 14.5$ ) of AAV-shControl (Figure 3aii).

However, this was not reflected in a reduction in vimentin levels, as assessed by IHC (Figure 3ciii,iv). Given that vimentin is stably expressed within the normal P10 retina (Figure 3bi), we reasoned that it might take longer for the knockdown in *Vimentin* RNA to be reflected in a change in vimentin protein levels (Desciaux et al., 2015). We compared untreated, AAV-shControl-treated and AAV-shVim-treated eyes at 6 weeks post-transduction (7.5 weeks of age). Vimentin levels were largely unchanged or increased in the untreated (Figure 3biv) and AAV-shControl treated (Figure 3di,ii) 7.5-week-old *Rho*<sup>-/-</sup> retina. In contrast, vimentin was markedly reduced in AAV-shVim expressing cells (Figure 3diii-iv). ShGfap did not result in any indirect effects on *Vimentin* expression (Figure 3aii). Taken together, these data show that administration of AAV-shGfap and AAV-shVim prevent the up-regulation of GFAP and vimentin, respectively, which is associated with progressive retinal degeneration in the mouse retina. As before, there was no indication of compensatory changes in the expression of the other IF (Figures 2aii and 3aii).

### 3.3 | Simultaneous knockdown of Gfap and Vimentin has deleterious effects on both degenerating and normal retina

We had sought to determine the effects of double knockdown of both *Gfap* and *Vimentin* using AAV-lh. However, despite achieving substantial knockdown of both *Gfap* and *Vimentin* in primary Müller glial cultures, AAV-lh failed to knockdown *Vimentin* in vivo (Figure 3aii, cv,vi, dv,vi). We therefore assessed the effects of introducing a mix of AAV-shGfap and AAV-shVim (i.e., double the total amount of vector) and compared the effect of this combined application with that of titer-matched AAV-shControl (Figure 4). Simultaneous knockdown of GFAP and vimentin together led to marked abnormalities in a significant proportion of treated retinæ; these included exacerbated degeneration and a failure to develop, leading to either anophthalmia or severe microphthalmia. In *Rho*<sup>-/-</sup> mice, 68% exhibited anophthalmia and 32% presented with microphthalmia ( $N = 9$  eyes; Figure 4a). In the microphthalmic eyes, transduction was patchy, but both GFAP and vimentin were reduced in regions of good DsRed expression by 6 weeks post-injection (Figure 4b). This was associated with a small, but significant reduction in ONL thickness

**FIGURE 3** RNAi targeting vectors mediate knockdown of vimentin in Müller glia in vivo in the degenerating retina. (ai) Histogram show that *Vimentin* mRNA levels, as assessed by RT-qPCR, are already abundant at the time of injection (P10) and increase significantly with degeneration. Administration of AAV-shControl vector had no effect on this increase. (ii) Administration of AAV-shVim led to a significant decrease in *Vimentin* mRNA at 3 weeks post-transduction (4.5 weeks of age), compared to AAV-shControl while no off-target effects were seen with AAV-shGfap. In contrast to the results in vitro, AAV-lh did not significantly reduce *Vimentin* mRNA in vivo.  $p < .05 = *$ ,  $p < .01 = **$ ,  $p < .001 = ***$  with a one-way ANOVA with Tukey's for multiple comparisons; Error bars: SD;  $n \geq 5$  independent retinæ per group. (b) Immunohistochemistry shows that vimentin (green) expression is widespread in Müller glia in both P10 (i) wild-type and (ii-iv) *Rho*<sup>-/-</sup> animals. (ci-iv) Examination of the retinæ injected with RNAi targeting vectors (red) showed that, at 3 weeks post-injection, there were no notable changes in Vimentin expression in any of the three conditions, compared to untreated age-matched eyes. (di-iv) Examination 6 weeks post-injection showed that vimentin expression remained robust in (i,ii) AAV-shControl treated eyes but was significantly reduced in transduced cells (red) in eyes treated with (iii,iv) AAV-shVim. (v,vi) No marked differences in vimentin expression were observed in eyes receiving AAV-lh. Retinal cryosections were counterstained with nuclei marker Hoechst 33342 (blue). GCL, ganglion cell layer; INL, inner nuclear layer; ONL, outer nuclear layer. Scale bar: 25  $\mu$ m [Color figure can be viewed at [wileyonlinelibrary.com](http://wileyonlinelibrary.com)]



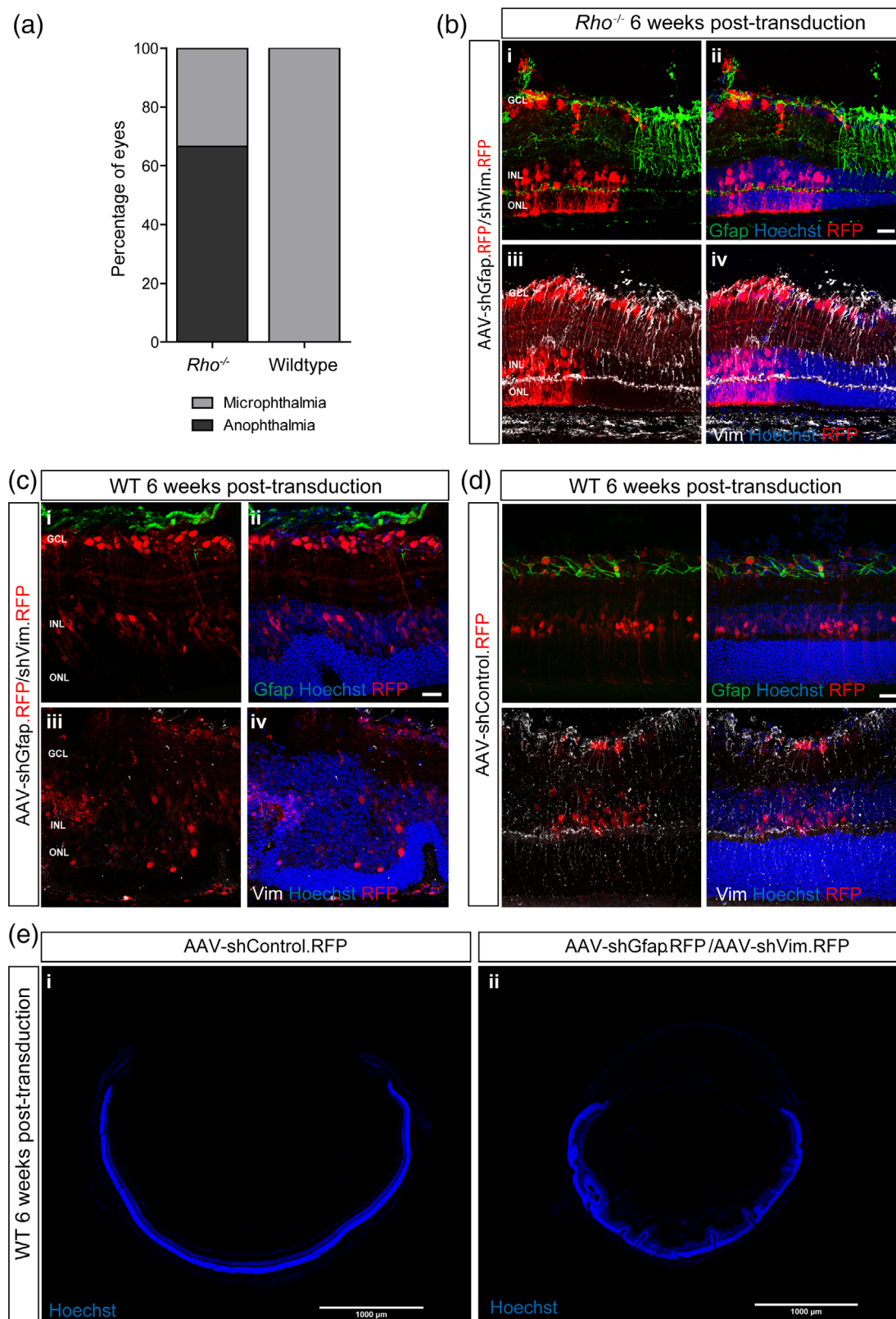


**FIGURE 4** Simultaneous knockdown of *Gfap* and *Vimentin* causes significant histological abnormalities in both degenerating and wild-type mice. (a–c) Confocal projections images of GFAP and Vimentin expression following co-administration of AAV-shGfap and AAV-shVim (1:1 ratio) into the same eye (a, c), or an equivalent titer of AAV-shCtrl (b). Images in (a, b) are from wild-type mice, while (c) shows *Rho*<sup>-/-</sup>. All images are 6 weeks post-injection. At both (a) 3 and (b) 6 weeks post-injection, a marked decrease in Gfap levels (green) was observed in transduced Müller glia cells (red). As before, Vimentin expression (grey) was largely unchanged at 3 weeks, but significantly reduced by 6 weeks, in transduced Müller glia. Retinal cryosections were counterstained with nuclei marker Hoechst 33342 (blue). GCL, ganglion cell layer; INL, inner nuclear layer; ONL, outer nuclear layer. Scale bar: 25  $\mu$ m. (c) In the majority of eyes, co-administration of these two vectors led to a failure to develop and resorption of the eye [Color figure can be viewed at [wileyonlinelibrary.com](http://wileyonlinelibrary.com)]

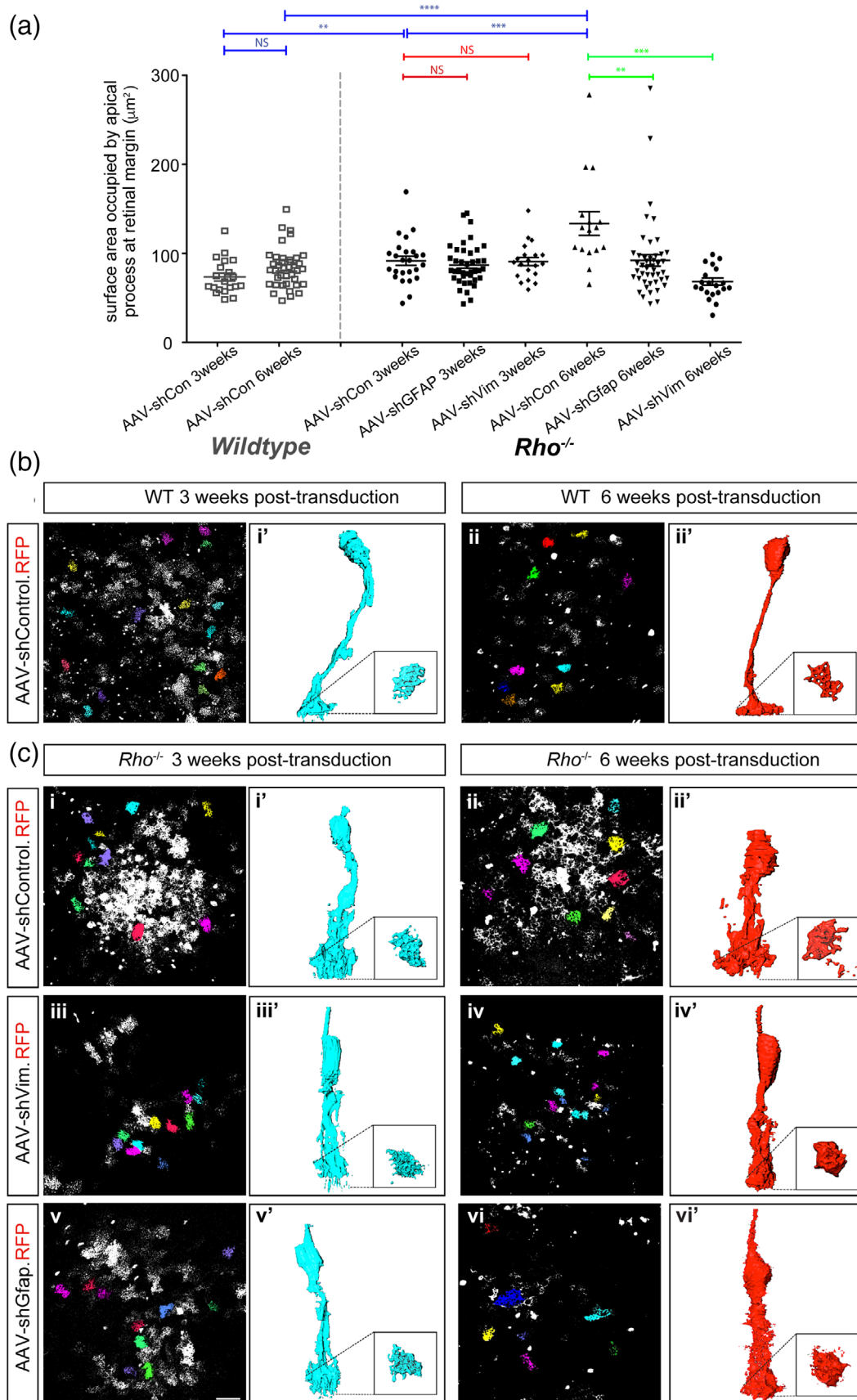


FIGURE 5 Legend on next page.

and number of photoreceptor rows (see Figure 6ai). Importantly, even in the absence of degeneration, we observed a similarly detrimental effect following co-injection of shGfp and shVim into wild-type eyes; 100% eyes ( $N = 8$ ; Figure 4a) were microphthalmic and presented very disturbed cytoarchitecture, including extensive whorl formation (Figure 4c,e). Qualitatively, the presence of whorls was typically associated with higher levels of transduction, as measured by DsRed expression in the combined knockdown (Figure S3a). To control for the increased viral load, we injected wild-type and  $Rho^{-/-}$  mice with volume and titer-matched AAV-shControl; neither group showed any such disturbances regardless of expression levels (Figure 4d,e; Figure S3b), indicating that this is a specific consequence of the absence of two principal IF proteins in the degenerating retina. This implies that there is a fundamental need for having at least one of these two IFs present, even in the absence of retinal degeneration, and points towards a role for compensatory increases in other IFs in constitutive double knockout models.

### 3.4 | Inhibiting degeneration-associated upregulation of either Gfap or Vimentin prevents Müller Glial hypertrophy in the $Rho^{-/-}$ retina but cannot reverse it once established

We next sought to determine what impact preventing the upregulation of individual IFs had on Müller glial cell hypertrophy in degeneration, as assessed by changes in morphology. By using serial reconstructions of individual, virally labeled Müller glia, we assessed the extent of lateral spread of their terminal processes at the apical margin of the neural retina, at the level of the OLM, together with their gross morphology (Figure 5). Examination of the overall morphology of AAV-shControl labeled Müller glial cells showed a marked increase in the thickness of the apical process and enlargement of the whole apical terminal region in  $Rho^{-/-}$  Müller glial cells, compared with age-matched wild-type controls. In wild-type retinæ, the lateral spread achieved by Müller glial apical terminal processes was  $73.4 \mu\text{m}^2$  ( $\pm 19.7$ ) and  $81.96 \mu\text{m}^2$  ( $\pm 19.8$ ) at 3 and 6 weeks of age, respectively (N.S.; Figure 5a,bi,ii). Müller glial lateral spread in  $Rho^{-/-}$  retina was already significantly larger at 3 weeks of age (1.2-fold increase;  $90.1 \mu\text{m}^2 \pm 20.5$ ;  $p < .01$ ) and increased further by 6 weeks

(1.5-fold increase;  $125.6 \mu\text{m}^2 \pm 36.8$ ;  $p < .0001$ ) compared to age-matched AAV-shControl treated WT (Figure 5a,ci,ii). These results indicate that marked and rapid changes in Müller glial cell hypertrophy occur at the apical margin of the retina between 3 and 6 weeks of age in the  $Rho^{-/-}$  model of retinal degeneration.

We then examined the impact of Gfap or Vimentin knockdown on Müller glial hypertrophy apical terminal process spread. As expected, no significant changes in lateral spread were observed at 3 weeks post-transduction of AAV-shGfap ( $88.5 \mu\text{m}^2 \pm 23.3$ , compared to  $90.1 \mu\text{m}^2 \pm 20.5$  in AAV-shControl-treated  $Rho^{-/-}$  cells; N.S.). However, by 6 weeks post-injection, AAV-shGfap transduced Müller cells presented a lateral spread ( $86.2 \mu\text{m}^2 \pm 24.2$ ) that was very similar to age-matched wild-type retinæ, and significantly reduced compared to shControl-treated  $Rho^{-/-}$  retinæ at the same time point ( $p < .001$ ; Figure 5aii). We observed an even larger difference in AAV-shVim treated cells; here, lateral spread was significantly reduced (–1.9-fold reduction;  $67.8 \mu\text{m}^2 \pm 17.7$ ;  $p < .001$ ) compared to age-matched AAV-shControl treated  $Rho^{-/-}$ , and the cells retained a gross morphology similar to age-matched wild-type AAV-shControl treated Müller glia (Figure 5aii, cii, iv), at 6 weeks post-transduction. As before, this difference was not apparent at the earlier, 3 week time point ( $92.4 \mu\text{m}^2 \pm 20.9$  in AAV-shVim treated cells; N.S.).

Although Gfap is expressed at very low levels by Müller glia in the normal, non-degenerating mammalian retina, Vimentin is always present and robustly expressed. We thus examined whether if knocking down either IF, but particularly vimentin, affected Müller glial morphology in the wild-type retina. P10 wild-type mice received AAV-shControl, AAV-shGfap or AAV-shVim and were examined 6 weeks post-injection. In all cases, no significant differences were observed, either in overall morphology or in apical spread, between AAV-shControl treated eyes and those receiving AAV-shVim or AAV-shGfap at either administration time point (Figure S4a). Together, these results demonstrate that knockdown of either Vimentin or Gfap prevents one of the most striking changes in Müller glial morphology associated with retinal degeneration, the establishment of hypertrophy, without adversely affecting Müller glial morphology in the normal retina.

We next sought to determine whether it is possible to modify hypertrophy once it is established.  $Rho^{-/-}$  or wild-type mice were injected at 4.5 weeks of age, when GFAP and vimentin expression is

**FIGURE 5** Vimentin is required for degeneration-associated hypertrophy of Müller glial apical processes. (a) Scatter plots show the area occupied by the apical terminal processes of Müller glia in  $Rho^{-/-}$  and wild-type animals transduced with AAV-shControl. At 4.5 weeks of age (i.e., 3 weeks post-transduction) there were no significant differences between the two strains, but at 7.5 weeks old (6 weeks post-transduction)  $Rho^{-/-}$  Müller glial apical terminal processes were hypertrophic and occupied a significantly larger area, compared to Müller glia in both 4.5 week old  $Rho^{-/-}$  and 7.5 week old wild-type controls. Comparison of the three RNAi vectors at 3 and 6 weeks post-transduction of  $Rho^{-/-}$  retinæ showed that AAV-shVim or AAV-shGfap each prevent the increase in area occupied by Müller glial apical terminal processes (red significance bars).  $p < .001 = ***$  and  $p < .0001 = ****$ , Statistical test applied, nonparametric t-test (blue); one-way ANOVA with posttest for multiple comparisons (red, for 3 week time point; green, for 6 week time point). Error bars: SD;  $n \geq 3$  independent retinæ per group. (bi,ii) Representative confocal images of analyzed apical surface areas and (bi', ii') representative examples of 3D reconstructed wild-type Müller glia at 3 and 6 weeks post-transduction with AAV-shControl. (ci–v) Representative confocal images of analyzed apical surface areas and (ci'–v') typical examples of 3D reconstructed  $Rho^{-/-}$  Müller glia at 3 and 6 weeks post-transduction with (i,ii) AAV-shControl, (iii, iv) AAV-shVim, and (v) AAV-shGfap. Scale bar: 20  $\mu\text{m}$  [Color figure can be viewed at [wileyonlinelibrary.com](http://wileyonlinelibrary.com)]



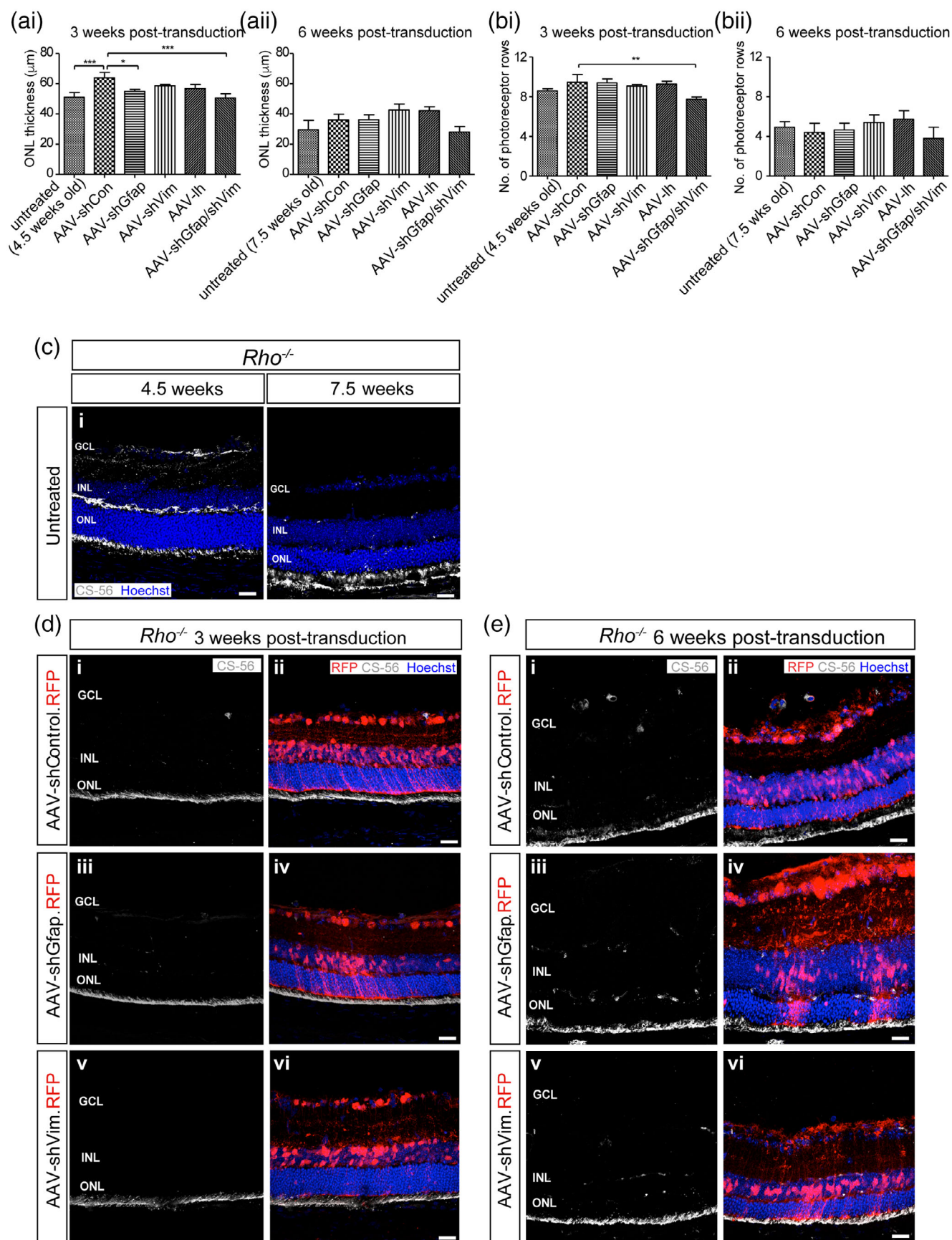


FIGURE 6 Legend on next page.



already upregulated, and examined 6 weeks later (Figure S4b,d). Transduction efficiency is lower following intravitreal injection into adult mice (Figure S4c), compared with P10 recipients, reducing the total number of cells that could be analyzed. However, we saw no reduction in apical spread in either shGfap- (1.02-fold change; N.S.) or shVim-treated (−1.03-fold change; N.S.) compared to shControl-treated *Rho*<sup>−/−</sup> retinas (*N* > 3 retinas for all conditions). Together, this suggests that reducing the expression of IFs alone may not be sufficient to reverse hypertrophy, once it has established.

### 3.5 | Preventing Müller glial hypertrophy in the *Rho*<sup>−/−</sup> retina does not alter photoreceptor cell death or gliosis-related changes in the extracellular matrix

As well as impeding Müller glial hypertrophy, we asked if preventing the upregulation of *Gfap* or *Vimentin* (transduction at P10) in the degenerating retina influenced other aspects of gliosis and/or photoreceptor degeneration. We first examined whether prevention of glial hypertrophy had a secondary effect on photoreceptor loss, either slowing it down or indeed exacerbating it (Figure 6a). No gross morphological changes in retinal architecture were observed following the knockdown of either *Gfap* or *Vimentin*. Accordingly, ONL thickness (Figure 6a) and the number of photoreceptor rows (Figure 6b) in AAV-shGfap or AAV-shVim treated were similar to that in untreated age-matched *Rho*<sup>−/−</sup> controls at both time points examined.

Upregulation of GFAP during gliosis is also typically associated with an increase in the production, by reactive Müller glia, of CSPGs and other related ECM molecules. We therefore examined whether preventing the upregulation of GFAP and vimentin levels and the associated glial hypertrophy had any secondary effect on CSPG deposition (Figure 6c,d). Staining for CS-56, a broad-spectrum marker of CSPGs, showed a modest increase in expression between 4.5 and 7.5 weeks of age in the untreated *Rho*<sup>−/−</sup> retina (Figure 6c) similar to our previous observations for this model (Hippert et al., 2015). However, no differences were observed between eyes treated with any of the RNAi vectors at either time point (Figure 6d,e), indicating that changes in the levels of *Gfap* and *Vimentin* do not influence significantly the production of CSPGs by reactive Müller glia.

## 4 | DISCUSSION

Glial scars, the cellular changes that constitute a physical barrier between the region of damage and the surrounding tissue, can be beneficial and protect the healthy tissue from the damaged environment, but they are also recognized as a major obstacle for neuronal repair (Burns & Stevens, 2018; Escartin, Guillemaud, & Carrillo-de Sauvage, 2019). In the context of regenerative medicine, they are hypothesized to impede endogenous repair mechanisms (Burns & Stevens, 2018) and represent a barrier to efficient connectivity between tissue grafts and implant devices and the host tissue, as well as reducing the efficiency of cell and gene therapy approaches (Hippert, Graca, & Pearson, 2016; Pearson, 2014). We must identify which aspects of scar formation are most problematic for the different types of regenerative therapy. Moreover, understanding scar formation is essential for developing strategies to ameliorate the negative consequences of scarring. Here, we show that the IFs vimentin and GFAP each play crucial roles in the establishment of reactive Müller glial cell hypertrophy and that preventing the upregulation of either, but particularly vimentin, can retain a Müller glial morphology similar to wild type in the progressively degenerating retina.

Although vimentin is the predominant IF protein expressed by both immature retinal progenitors and normal adult Müller glial cells, GFAP has received most attention due to its striking upregulation following injury (Messing & Brenner, 2020). This upregulation has been postulated to help form and stabilize the hypertrophic cellular processes exhibited by reactive astrocytes and glia, which represent the most striking morphological change associated with glial scarring (Lundkvist et al., 2004; Verardo et al., 2008). However, this notion remains an area of significant debate, due to numerous conflicting reports of attempts to manipulate glial IF expression and results from in vitro studies have often differed from those obtained in vivo (reviewed in Pekny, Wilhelmsson, Tatlisumak, & Pekna, 2019; Wilhelmsson et al., 2017; Zeisel et al., 2018), underlining the importance of testing gliosis in context. Indeed, in our study, knockdown of vimentin led to little or no changes in the morphology of Müller glia in vitro, but almost completely prevented degeneration-induced Müller glial hypertrophy in vivo. Such differences exemplify not only the regional differences in the role of IFs, but also the importance of the cytoarchitectural context when assessing the role of a given IF.

**FIGURE 6** Suppression of gliosis-related upregulation of GFAP and vimentin does not affect photoreceptor degeneration or CSPG deposition. (a) Administration of AAV RNAi vectors by intravitreal injection resulted in little or no changes to ONL thickness, compared to non-injected age-matched controls, at (i) 3, or (ii) 6 weeks post-injection. (b) Administration of AAV RNAi vectors by intravitreal injection resulted in little or no changes to number of photoreceptor rows, compared to non-injected age-matched controls, at (i) 3 or (ii) 6 weeks post-injection, with the exception of a small, but significant, decrease in those eyes co-injected with AAV-shGfap and AAV-shVim at 3 weeks post transduction, compared to AAV-shControl treated eyes.  $p < .05 = *$ ,  $p < .01 = **$ ,  $p < .001 = ***$ , with a one-way ANOVA with correction for multiple comparisons. Error bars: SD;  $n \geq 5$  independent retinas per group. N.B. a small but significant increase in ONL thickness was seen at 3, but not 6, weeks post-injection of AAV-shControl treated *Rho*<sup>−/−</sup> retinas, compared to age-matched untreated eyes; this likely reflects an injection-related disturbance, since no difference was observed in the number of photoreceptor rows. (c) CSPG expression (as shown by CS-56 staining; grey) increases between 4.5 and 7.5 weeks of age in the degenerating *Rho*<sup>−/−</sup> retina. (d,e) Administration of AAV RNAi vectors (red) by intravitreal injection at P10 resulted in little or no changes to ONL thickness, compared to non-injected age-matched controls, at (d) 3 weeks or (e) 6 weeks post-injection. Scale bar: 25  $\mu$ m [Color figure can be viewed at [wileyonlinelibrary.com](http://wileyonlinelibrary.com)]



A further limitation of preceding investigations has been the reliance on knockout models, in which the protein in question is absent from the point of conception onwards and the development of that animal may be subject to multiple compensatory mechanisms. Given that GFAP has been known of for more the 50 years, it is perhaps surprising that relatively few studies have sought to manipulate its expression (or that of vimentin) after development is complete (Messing & Brenner, 2020). Moreover, the majority of studies have focused on non-degenerative models, meaning that assessments of the role played by different IFs invariably reflect their role in the glial response to acute trauma, rather than to progressive degenerative injuries (Burda & Sofroniew, 2014).

To begin to address these issues, we designed an *in vivo* gene silencing strategy to intervene in glial hypertrophy at different time points in the progressively degenerating retina, based on RNAi-mediated inhibition of *Gfap* and/or *Vimentin*. We report that expression of *Gfap* and *Vimentin* can be effectively suppressed in the intact degenerating retina and that this can markedly influence Müller glial morphology at the apical margin of the neural retina. Specifically, suppression of either *Gfap* or *Vimentin* expression prevented Müller glial cells undergoing hypertrophy in response to progressive photoreceptor degeneration, meaning that the cells retained morphologies similar to wild-type Müller glial cells. Our findings support the hypothesized role for GFAP in establishing Müller glial cell hypertrophy in progressive degeneration. They are also consistent with recent reports applying the related strategy of antisense oligonucleotides against GFAP, which suppressed the expression of GFAP and the formation of Rosenthal fibers in another progressive neuronal degeneration, Alexander's Disease (Hagemann et al., 2018). These studies contrast with early reports of the glial response to an acute needle stab injury in either the cortex or spinal cord in *Gfap*<sup>-/-</sup> knockout models, which was indistinguishable between *Gfap*<sup>-/-</sup> and wild-type mice (Pekny et al., 1995; Pekny et al., 1999).

However, it is the role of vimentin that is most striking. Our data indicate a key role for vimentin in the structural changes associated with Müller glial hypertrophy as part of retinal glial scar formation. This notion is supported by early studies by Lewis and Fisher in the feline retina, where only vimentin<sup>+</sup> Müller glial processes grew into the subretinal space and formed the scar occurring following retinal detachment (Fisher & Lewis, 2003; Lewis & Fisher, 2000). Additional support comes from studies on the ground squirrel retina: In this species, Müller glia do not upregulate the expression of *Gfap* following retinal detachment, however, *Vimentin* expression increases in the Müller glial terminal processes around surviving photoreceptors (Linberg, Sakai, Lewis, & Fisher, 2002; Merriman, Sajdak, Li, & Jones, 2016). In these retinas, despite the lack of GFAP upregulation, vimentin<sup>+</sup> Müller glial processes apparently still filled the empty spaces left by dead photoreceptors, preserving gross retinal structure. In the absence of vimentin, it will be interesting to explore the composition of the intercellular space in hypertrophic and AAV-shVim-treated diseased retina using serial section electron microscopy.

Vimentin's role in hypertrophy may explain the surprisingly mild effects of knocking out *Gfap* observed in earlier reports. Vimentin

filaments are absent in astrocytes in the uninjured corpus callosum, spinal cord and hippocampus of *Gfap*<sup>-/-</sup> mice but *Vimentin* expression is markedly increased following injury or culturing of *Gfap*<sup>-/-</sup> astrocytes, suggesting an attempt to compensate for the lack of GFAP (Eliasson et al., 1999). In uninjured *Gfap*<sup>-/-</sup> mice, vimentin filaments are seen in the anterior column of the cervical spinal cord (X. Wang, Messing, & David, 1997), in cerebellar Bergmann glia (Galou et al., 1996) and in Müller cells in the retina (Gomi et al., 1995). In *Vim*<sup>-/-</sup> mice, reactive brain astrocytes can still form IFs but they are comprised of abnormally tightly packed GFAP bundles (Eliasson et al., 1999), in keeping with the notion that vimentin acts as a facilitator of GFAP filament assembly (Galou et al., 1996). Vimentin itself also requires a partner for polymerization, but in the absence of GFAP, this can be other IF proteins, such as nestin or synemin. Surprisingly, however, other studies of *Vim*<sup>-/-</sup> mice have shown that in the injured brain, astrocytes are able to form some abnormal IFs, but these are made only of GFAP, and that loss of vimentin was associated with a decrease in nestin and synemin protein expression (Eliasson et al., 1999). It would, therefore, appear that potential compensatory changes associated with knockout of a given IF(s) are complex and context dependent. Further studies are required to determine whether there are compensatory changes in the expression of other IFs in response to knockdown of vimentin and/or *Gfap* in the intact progressively degenerating retina. These might include the development of an inducible knockout system on a retinal degeneration background, where *Vimentin* and *Gfap* might be knocked out at specific time points in development, adulthood and during the disease process. Regardless, these data, together with the findings reported here that Müller glial hypertrophy is significantly impeded by the removal of vimentin, reveal an under-appreciated role played by vimentin in the structural changes associated with reactive gliosis.

If prolonged, glial scarring is understood to exacerbate neuronal degeneration. It is not clear, however, if the converse is true, that is, whether prevention or reduction in glial scarring has any beneficial effect on neuronal degeneration. Miller and colleagues (Nakazawa et al., 2007) reported that chemical or detachment-induced retinal degeneration was less extensive in *Gfap*<sup>-/-</sup>/*Vim*<sup>-/-</sup> mice compared to wild-type controls, while Sivak and colleagues (Livne-Bar et al., 2016) reported that blockade of Type III IF dynamics (which includes GFAP and vimentin) using Withaferin A led to a reduction in metabolic injury-induced inner retinal apoptosis. By contrast, Perez and colleagues (Wunderlich et al., 2015) noted that cell death was accelerated in the inner retina in *Gfap*<sup>-/-</sup>/*Vim*<sup>-/-</sup> mice after ischemia/reperfusion, but that photoreceptor cell loss was comparable to that in wild-type mice. Here, we found that the degree of photoreceptor loss associated with progressive retinal degeneration was largely unaffected by RNAi-mediated suppression of GFAP or vimentin alone. However, simultaneous knockdown of both *Gfap* and *Vimentin* in both the degenerating *Rho*<sup>-/-</sup> and in the normal wild-type retina resulted in severe abnormalities, with many injected eyes failing to develop normally. This may be explained by the fact that when both are removed, functional IFs cannot form since other IFs, such as nestin (Eliasson et al., 1999) or synemin (Jing et al., 2007), are able to form



IFs alone. As discussed earlier, differences between knockout and RNAi approaches may be explained in part by compensatory mechanisms that come into play in the knockout, which would otherwise not be present in a normal developing/diseased retina. In those retinæ that did go on to develop following GFAP/vimentin knockdown using RNAi, a small exacerbation of photoreceptor loss was observed, indicating a dose-dependent effect. Taken together, these findings indicate that reducing either GFAP or vimentin alone does not ameliorate (nor exacerbate) photoreceptor loss during progressive degeneration. They also suggest that the impact of IF deficiency on retinal cell survival is both disease- and cell type-specific.

There is a growing body of evidence demonstrating the negative consequences of reactive gliosis, particularly when it is not resolved within the post-acute phase after injury. While the acute response may ensure the survival of cells through the post-traumatic phase, prolonged gliosis and scarring have negative effects on regeneration and plasticity, as shown in a range of different experimental models (reviewed in Pekny & Pekna, 2014). The stiffness of glial cells, which correlates with IF expression, is proposed to affect the regenerative properties of nervous tissue (Lu et al., 2011; Moeendarbary et al., 2017; L. Wang et al., 2018). Reducing hypertrophy, as one aspect of gliosis, may therefore provide a more permissive environment for regeneration. Indeed, *Gfap*<sup>-/-</sup>/*Vim*<sup>-/-</sup> mice showed reduced hypertrophy of astrocytes and a partial restoration of synaptic connectivity after entorhinal cortex lesion (Wilhelmsson et al., 2004). Similarly, extensive sprouting was observed in *Gfap*<sup>-/-</sup>/*Vim*<sup>-/-</sup> mice after spinal cord hemi-section and these animals also performed better in behavioral tasks (Menet, Prieto, Privat, & Gimenez y Ribotta, 2003). Interestingly, *Gfap*<sup>-/-</sup> animals performed similar to wild type and did not show any improvement regarding neurite sprouting and outgrowth or function, again underlining the importance of vimentin in this process. There is much excitement around the potential for Müller glial cell cycle re-entry and Müller glial-mediated endogenous repair of the retina, a phenomenon common in lower vertebrates, but rarely seen in the mammalian retina (see (Langhe & Pearson, 2020; Pearson & Ali, 2018) and it will be of significant interest to explore the role of Müller glial-stiffness in modulating this response.

Novel therapeutic approaches include the subretinal and intravitreal transplantation of various donor cell populations (Aghaizu, Kruczek, Gonzalez-Cordero, Ali, & Pearson, 2017; Barber et al., 2013; Barnea-Cramer et al., 2016; Kruczek et al., 2017; Pearson et al., 2012; Tassoni et al., 2015; Waldron et al., 2018) and neonatal (Seiler & Aramant, 2012) and stem cell-derived (Mandai et al., 2017) retinal sheet grafts and the introduction of subretinal and epiretinal electronic implants (Pardue et al., 2001; Zrenner et al., 2011). Each of these requires close physical interaction between the graft and the remaining host inner retina, where extensive hypertrophy at the apical surface of the neural retina may impede (Hippert et al., 2016). Further investigations are required to determine the relative contributions of glial hypertrophy and gliosis-related changes in ECM composition on the efficacy of these different therapeutic approaches. Although we did not see a beneficial effect of attenuating glial hypertrophy on photoreceptor loss directly, it may still be of indirect benefit to patients

with progressive retinal degeneration. For example, gliosis is common in patients with diabetic retinopathy (Lechner, O'Leary, & Stitt, 2017; Mizutani, Gerhardinger, & Lorenzi, 1998) and may contribute to pathogenesis; for example, diabetic retinopathy is frequently exacerbated by glial hypertrophy at the vitreal and apical surfaces of the retina leading to retinal detachment. In the current study, we were able to almost completely prevent Müller Glial hypertrophy, at least at the apical surface (we did not examine hypertrophy at the vitreal surface), raising the possibility of designing therapeutic approaches that might at least partially ameliorate this condition. Notably, however, we could not reverse hypertrophy by RNAi once it was established, underlining the importance of correct, and most likely early, timing for any such interventions.

Together, our findings deepen our understanding of the roles played by different IFs in the complex process of gliosis, highlighting the importance of vimentin in establishing glial hypertrophy and open new therapeutic avenues for potentially ameliorating this aspect of glial scarring in retinal and CNS degeneration.

## ACKNOWLEDGMENTS

We thank the UCL IoO vector production facility for technical support, Y. Duran, L. Abelleira-Hervas, J. Hoke and A. Hare for assistance in animal husbandry and members of the Gene and Cell Therapy Group for constructive discussion during the project. This work was supported by the Royal Society (UF120046; RG080398); Moorfields Eye Charity (E170004A; R150032A, R180005A); Fight for Sight (1448/1449; 1566-1567); Retina UK (GR566); Medical Research Council UK (MR/J004553/1; MR/T002735/1). A.G. was an MRC 4 year Clinical Neuroscience PhD student, A.A.K was a Fight for Sight-funded Frankenburg PhD student, N.A. was a UCL Grand Challenge PhD student. Graphical abstract created using BioRender.com

## CONFLICT OF INTERESTS

The authors declare no conflict of interests.

## DATA AVAILABILITY STATEMENT

The data that support the findings of this study are available from the corresponding author upon reasonable request.

## ORCID

Joana Ribeiro <https://orcid.org/0000-0002-9290-6023>

Rachael A. Pearson <https://orcid.org/0000-0002-1107-1969>

## REFERENCES

- Aghaizu, N. D., Kruczek, K., Gonzalez-Cordero, A., Ali, R. R., & Pearson, R. A. (2017). Pluripotent stem cells and their utility in treating photoreceptor degenerations. *Progress in Brain Research*, 231, 191–223. <https://doi.org/10.1016/bs.pbr.2017.01.001>
- Barber, A. C., Hippert, C., Duran, Y., West, E. L., Bainbridge, J. W., Warre-Cornish, K., ... Pearson, R. A. (2013). Repair of the degenerate retina by photoreceptor transplantation. *Proceedings of the National Academy of Sciences of the United States of America*, 110(1), 354–359. <https://doi.org/10.1073/pnas.1212677110>

- Barnea-Cramer, A. O., Wang, W., Lu, S. J., Singh, M. S., Luo, C., Huo, H., ... Lanza, R. (2016). Function of human pluripotent stem cell-derived photoreceptor progenitors in blind mice. *Scientific Reports*, 6, 29784. <https://doi.org/10.1038/srep29784>
- Bringmann, A., Pannicke, T., Grosche, J., Francke, M., Wiedemann, P., Skatchkov, S. N., ... Reichenbach, A. (2006). Muller cells in the healthy and diseased retina. *Progress in Retinal and Eye Research*, 25(4), 397–424. <https://doi.org/10.1016/j.preteyeres.2006.05.003>
- Burda, J. E., & Sofroniew, M. V. (2014). Reactive gliosis and the multicellular response to CNS damage and disease. *Neuron*, 81(2), 229–248. <https://doi.org/10.1016/j.neuron.2013.12.034>
- Burns, M. E., & Stevens, B. (2018). Report on the National eye Institute's audacious goals initiative: Creating a cellular environment for neuroregeneration. *eNeuro*, 5(2), ENEURO.0035-18.2018. <https://doi.org/10.1523/ENEURO.0035-18.2018>
- Calame, M., Cachafeiro, M., Philippe, S., Schouwey, K., Tekaya, M., Wanner, D., ... Arsenijevic, Y. (2011). Retinal degeneration progression changes lentiviral vector cell targeting in the retina. *PLoS One*, 6(8), e23782. <https://doi.org/10.1371/journal.pone.0023782>
- Chan, C. C., Wong, A. K., Liu, J., Steeves, J. D., & Tetzlaff, W. (2007). ROCK inhibition with Y27632 activates astrocytes and increases their expression of neurite growth-inhibitory chondroitin sulfate proteoglycans. *Glia*, 55(4), 369–384. <https://doi.org/10.1002/glia.20466>
- Chen, L. F., FitzGibbon, T., He, J. R., & Yin, Z. Q. (2012). Localization and developmental expression patterns of CSPG-cs56 (aggrecan) in normal and dystrophic retinas in two rat strains. *Experimental Neurology*, 234(2), 488–498. <https://doi.org/10.1016/j.expneurol.2012.01.023>
- Cregg, J. M., DePaul, M. A., Filous, A. R., Lang, B. T., Tran, A., & Silver, J. (2014). Functional regeneration beyond the glial scar. *Experimental Neurology*, 253, 197–207. <https://doi.org/10.1016/j.expneurol.2013.12.024>
- Desclaux, M., Perrin, F. E., Do-Thi, A., Prieto-Cappellini, M., Gimenez, Y. R. M., Mallet, J., & Privat, A. (2015). Lentiviral-mediated silencing of glial fibrillary acidic protein and vimentin promotes anatomical plasticity and functional recovery after spinal cord injury. *Journal of Neuroscience Research*, 93(1), 43–55. <https://doi.org/10.1002/jnr.23468>
- Eliasson, C., Sahlgren, C., Berthold, C. H., Stakeberg, J., Celis, J. E., Betsholtz, C., ... Pekny, M. (1999). Intermediate filament protein partnership in astrocytes. *The Journal of Biological Chemistry*, 274(34), 23996–24006. <https://doi.org/10.1074/jbc.274.34.23996>
- Escartin, C., Guillemaud, O., & Carrillo-de Sauvage, M. A. (2019). Questions and (some) answers on reactive astrocytes. *Glia*, 67(12), 2221–2247. <https://doi.org/10.1002/glia.23687>
- Fawcett, J. W., & Curt, A. (2009). Damage control in the nervous system: Rehabilitation in a plastic environment. *Nature Medicine*, 15(7), 735–736. <https://doi.org/10.1038/nm0709-735>
- Fisher, S. K., & Lewis, G. P. (2003). Muller cell and neuronal remodeling in retinal detachment and reattachment and their potential consequences for visual recovery: A review and reconsideration of recent data. *Vision Research*, 43(8), 887–897. [https://doi.org/10.1016/s0042-6989\(02\)00680-6](https://doi.org/10.1016/s0042-6989(02)00680-6)
- Galou, M., Colucci-Guyon, E., Ensergueix, D., Ridet, J. L., Gimenez, Y., Ribotta, M., ... Dupouey, P. (1996). Disrupted glial fibrillary acidic protein network in astrocytes from vimentin knockout mice. *The Journal of Cell Biology*, 133(4), 853–863. <https://doi.org/10.1083/jcb.133.4.853>
- Gao, G. P., Alvira, M. R., Wang, L., Calcedo, R., Johnston, J., & Wilson, J. M. (2002). Novel adeno-associated viruses from rhesus monkeys as vectors for human gene therapy. *Proceedings of the National Academy of Sciences of the United States of America*, 99(18), 11854–11859. <https://doi.org/10.1073/pnas.182412299>
- Gomi, H., Yokoyama, T., Fujimoto, K., Ikeda, T., Katoh, A., Itoh, T., & Itoharu, S. (1995). Mice devoid of the glial fibrillary acidic protein develop normally and are susceptible to scrapie prions. *Neuron*, 14(1), 29–41. Retrieved from <http://www.ncbi.nlm.nih.gov/pubmed/7826639>
- Hagemann, T. L., Powers, B., Mazur, C., Kim, A., Wheeler, S., Hung, G., Swauze, E., & Messing, A. (2018). Antisense suppression of glial fibrillary acidic protein as a treatment for Alexander disease. *Annals of Neurology*, 83(1), 27–39. <https://doi.org/10.1002/ana.25118>
- Hamby, M. E., & Sofroniew, M. V. (2010). Reactive astrocytes as therapeutic targets for CNS disorders. *Neurotherapeutics*, 7(4), 494–506. <https://doi.org/10.1016/j.nurt.2010.07.003>
- Hippert, C., Graca, A. B., Barber, A. C., West, E. L., Smith, A. J., Ali, R. R., & Pearson, R. A. (2015). Muller glia activation in response to inherited retinal degeneration is highly varied and disease-specific. *PLoS One*, 10(3), e0120415. <https://doi.org/10.1371/journal.pone.0120415>
- Hippert, C., Graca, A. B., & Pearson, R. A. (2016). Gliosis can impede integration following photoreceptor transplantation into the diseased retina. *Advances in Experimental Medicine and Biology*, 854, 579–585. [https://doi.org/10.1007/978-3-319-17121-0\\_77](https://doi.org/10.1007/978-3-319-17121-0_77)
- Humphries, M. M., Rancourt, D., Farrar, G. J., Kenna, P., Hazel, M., Bush, R. A., ... Humphries, P. (1997). Retinopathy induced in mice by targeted disruption of the rhodopsin gene. *Nature Genetics*, 15(2), 216–219. <https://doi.org/10.1038/ng0297-216>
- Jadhav, A. P., Roesch, K., & Cepko, C. L. (2009). Development and neurogenic potential of Muller glial cells in the vertebrate retina. *Progress in Retinal and Eye Research*, 28(4), 249–262. <https://doi.org/10.1016/j.preteyeres.2009.05.002>
- Jing, R., Wilhelmsson, U., Goodwill, W., Li, L., Pan, Y., Pekny, M., & Skalli, O. (2007). Synemin is expressed in reactive astrocytes in neurotrauma and interacts differentially with vimentin and GFAP intermediate filament networks. *Journal of Cell Science*, 120(Pt 7), 1267–1277. <https://doi.org/10.1242/jcs.03423>
- Klimczak, R. R., Koerber, J. T., Dalkara, D., Flannery, J. G., & Schaffer, D. V. (2009). A novel adeno-associated viral variant for efficient and selective intravitreal transduction of rat Muller cells. *PLoS One*, 4(10), e7467. <https://doi.org/10.1371/journal.pone.0007467>
- Kruczek, K., Gonzalez-Cordero, A., Goh, D., Naem, A., Jonikas, M., Blackford, S. J. I., ... Ali, R. R. (2017). Differentiation and transplantation of embryonic stem cell-derived cone photoreceptors into a mouse model of end-stage retinal degeneration. *Stem Cell Reports*, 8(6), 1659–1674. <https://doi.org/10.1016/j.stemcr.2017.04.030>
- Langhe, R., & Pearson, R. A. (2020). Rebuilding the retina: Prospects for Muller glial-mediated self-repair. *Current Eye Research*, 45(3), 349–360. <https://doi.org/10.1080/02713683.2019.1669665>
- Lechner, J., O'Leary, O. E., & Stitt, A. W. (2017). The pathology associated with diabetic retinopathy. *Vision Research*, 139, 7–14. <https://doi.org/10.1016/j.visres.2017.04.003>
- Lewis, G. P., & Fisher, S. K. (2000). Muller cell outgrowth after retinal detachment: Association with cone photoreceptors. *Investigative Ophthalmology and Visual Science*, 41(6), 1542–1545. Retrieved from <https://www.ncbi.nlm.nih.gov/pubmed/10798674>
- Linberg, K. A., Sakai, T., Lewis, G. P., & Fisher, S. K. (2002). Experimental retinal detachment in the cone-dominant ground squirrel retina: Morphology and basic immunocytochemistry. *Visual Neuroscience*, 19(5), 603–619. <https://doi.org/10.1017/s095252380219506x>
- Livne-Bar, I., Lam, S., Chan, D., Guo, X., Askar, I., Nahirnyj, A., ... Sivak, J. M. (2016). Pharmacologic inhibition of reactive gliosis blocks TNF-alpha-mediated neuronal apoptosis. *Cell Death & Disease*, 7(9), e2386. <https://doi.org/10.1038/cddis.2016.277>
- Loffler, K., Schafer, P., Volkner, M., Holdt, T., & Karl, M. O. (2015). Age-dependent Muller glia neurogenic competence in the mouse retina. *Glia*, 63(10), 1809–1824. <https://doi.org/10.1002/glia.22846>
- Lu, Y. B., Iandiev, I., Hollborn, M., Korber, N., Ulbricht, E., Hirrlinger, P. G., ... Kas, J. A. (2011). Reactive glial cells: Increased stiffness correlates with increased intermediate filament expression. *The FASEB Journal*, 25(2), 624–631. <https://doi.org/10.1096/fj.10-163790>

- Lundkvist, A., Reichenbach, A., Betsholtz, C., Carmeliet, P., Wolburg, H., & Pekny, M. (2004). Under stress, the absence of intermediate filaments from Muller cells in the retina has structural and functional consequences. *Journal of Cell Science*, 117 (Pt 16), 3481–3488. <https://doi.org/10.1242/jcs.01221>
- Mandai, M., Fujii, M., Hashiguchi, T., Sunagawa, G. A., Ito, S. I., Sun, J., ... Takahashi, M. (2017). iPSC-derived retina transplants improve vision in rd1 end-stage retinal-degeneration mice. *Stem Cell Reports*, 8(1), 69–83. <https://doi.org/10.1016/j.stemcr.2016.12.008>
- Menet, V., Prieto, M., Privat, A., & Gimenez y Ribotta, M. (2003). Axonal plasticity and functional recovery after spinal cord injury in mice deficient in both glial fibrillary acidic protein and vimentin genes. *Proceedings of the National Academy of Sciences of the United States of America*, 100(15), 8999–9004. <https://doi.org/10.1073/pnas.1533187100>
- Merriman, D. K., Sajdak, B. S., Li, W., & Jones, B. W. (2016). Seasonal and post-trauma remodeling in cone-dominant ground squirrel retina. *Experimental Eye Research*, 150, 90–105. <https://doi.org/10.1016/j.exer.2016.01.011>
- Messing, A., & Brenner, M. (2020). GFAP at 50. *ASN Neuro*, 12, 1759091420949680. <https://doi.org/10.1177/1759091420949680>
- Mizutani, M., Gerhardinger, C., & Lorenzi, M. (1998). Muller cell changes in human diabetic retinopathy. *Diabetes*, 47(3), 445–449. <https://doi.org/10.2337/diabetes.47.3.445>
- Moeendarbary, E., Weber, I. P., Sheridan, G. K., Koser, D. E., Soleman, S., Haenzi, B., ... Franze, K. (2017). The soft mechanical signature of glial scars in the central nervous system. *Nature Communications*, 8, 14787. <https://doi.org/10.1038/ncomms14787>
- Nakazawa, T., Takeda, M., Lewis, G. P., Cho, K. S., Jiao, J., Wilhelmsson, U., ... Miller, J. W. (2007). Attenuated glial reactions and photoreceptor degeneration after retinal detachment in mice deficient in glial fibrillary acidic protein and vimentin. *Investigative Ophthalmology & Visual Science*, 48(6), 2760–2768. <https://doi.org/10.1167/iovs.06-1398>
- Pardue, M. T., Stubbs, E. B., Jr., Perlman, J. I., Narfstrom, K., Chow, A. Y., & Peachey, N. S. (2001). Immunohistochemical studies of the retina following long-term implantation with subretinal microphotodiode arrays. *Experimental Eye Research*, 73(3), 333–343. <https://doi.org/10.1006/exer.2001.1041>
- Pearson, R. A. (2014). Advances in repairing the degenerate retina by rod photoreceptor transplantation. *Biotechnology Advances*, 32(2), 485–491. <https://doi.org/10.1016/j.biotechadv.2014.01.001>
- Pearson, R. A., & Ali, R. R. (2018). Unlocking the potential for endogenous repair to restore sight. *Neuron*, 100(3), 524–526. <https://doi.org/10.1016/j.neuron.2018.10.035>
- Pearson, R. A., Barber, A. C., Rizzi, M., Hippert, C., Xue, T., West, E. L., ... Ali, R. R. (2012). Restoration of vision after transplantation of photoreceptors. *Nature*, 485(7396), 99–103. <https://doi.org/10.1038/nature10997>
- Pearson, R. A., Barber, A. C., West, E. L., MacLaren, R. E., Duran, Y., Bainbridge, J. W., ... Ali, R. R. (2010). Targeted disruption of outer limiting membrane junctional proteins (Crb1 and ZO-1) increases integration of transplanted photoreceptor precursors into the adult wild-type and degenerating retina. *Cell Transplantation*, 19(4), 487–503. <https://doi.org/10.3727/096368909X486057>
- Pearson, R. A., Hippert, C., Graca, A. B., & Barber, A. C. (2014). Photoreceptor replacement therapy: Challenges presented by the diseased recipient retinal environment. *Visual Neuroscience*, 31(4–5), 333–344. <https://doi.org/10.1017/S0952523814000200>
- Pekny, M., Johansson, C. B., Eliasson, C., Stakeberg, J., Wallen, A., Perlmann, T., ... Frisen, J. (1999). Abnormal reaction to central nervous system injury in mice lacking glial fibrillary acidic protein and vimentin. *The Journal of Cell Biology*, 145(3), 503–514. <https://doi.org/10.1083/jcb.145.3.503>
- Pekny, M., Leveen, P., Pekna, M., Eliasson, C., Berthold, C. H., Westermark, B., & Betsholtz, C. (1995). Mice lacking glial fibrillary acidic protein display astrocytes devoid of intermediate filaments but develop and reproduce normally. *EMBO Journal*, 14(8), 1590–1598. Retrieved from <https://www.ncbi.nlm.nih.gov/pubmed/7737111>
- Pekny, M., & Pekna, M. (2014). Astrocyte reactivity and reactive astrogliosis: Costs and benefits. *Physiological Reviews*, 94(4), 1077–1098. <https://doi.org/10.1152/physrev.00041.2013>
- Pekny, M., Wilhelmsson, U., & Pekna, M. (2014). The dual role of astrocyte activation and reactive gliosis. *Neuroscience Letters*, 565, 30–38. <https://doi.org/10.1016/j.neulet.2013.12.071>
- Pekny, M., Wilhelmsson, U., Tatlisumak, T., & Pekna, M. (2019). Astrocyte activation and reactive gliosis—A new target in stroke? *Neuroscience Letters*, 689, 45–55. <https://doi.org/10.1016/j.neulet.2018.07.021>
- Schildge, S., Bohrer, C., Beck, K., & Schachtrup, C. (2013). Isolation and culture of mouse cortical astrocytes. *Journal of Visualized Experiments*, 71, 50079. <https://doi.org/10.3791/50079>
- Seiler, M. J., & Aramant, R. B. (2012). Cell replacement and visual restoration by retinal sheet transplants. *Progress in Retinal and Eye Research*, 31(6), 661–687. <https://doi.org/10.1016/j.preteyeres.2012.06.003>
- Silver, J., & Miller, J. H. (2004). Regeneration beyond the glial scar. *Nature Reviews. Neuroscience*, 5(2), 146–156. <https://doi.org/10.1038/nrn1326>
- Tassoni, A., Gutteridge, A., Barber, A. C., Osborne, A., & Martin, K. R. (2015). Molecular mechanisms mediating retinal reactive gliosis following bone marrow mesenchymal stem cell transplantation. *Stem Cells*, 33(10), 3006–3016. <https://doi.org/10.1002/stem.2095>
- Vazquez-Chona, F. R., Clark, A. M., & Levine, E. M. (2009). Rlb1 promoter drives robust Muller glial GFP expression in transgenic mice. *Investigative Ophthalmology & Visual Science*, 50(8), 3996–4003. <https://doi.org/10.1167/iovs.08-3189>
- Verardo, M. R., Lewis, G. P., Takeda, M., Linberg, K. A., Byun, J., Luna, G., ... Fisher, S. K. (2008). Abnormal reactivity of muller cells after retinal detachment in mice deficient in GFAP and vimentin. *Investigative Ophthalmology & Visual Science*, 49(8), 3659–3665. <https://doi.org/10.1167/iovs.07-1474>
- Waldron, P. V., Di Marco, F., Kruczek, K., Ribeiro, J., Graca, A. B., Hippert, C., ... Pearson, R. A. (2018). Transplanted donor- or stem cell-derived cone photoreceptors can both integrate and undergo material transfer in an environment-dependent manner. *Stem Cell Reports*, 10(2), 406–421. <https://doi.org/10.1016/j.stemcr.2017.12.008>
- Wang, L., Xia, J., Li, J., Hagemann, T. L., Jones, J. R., Fraenkel, E., ... Feany, M. B. (2018). Tissue and cellular rigidity and mechanosensitive signaling activation in Alexander disease. *Nature Communications*, 9(1), 1899. <https://doi.org/10.1038/s41467-018-04269-7>
- Wang, X., Messing, A., & David, S. (1997). Axonal and nonneuronal cell responses to spinal cord injury in mice lacking glial fibrillary acidic protein. *Experimental Neurology*, 148(2), 568–576. <https://doi.org/10.1006/exnr.1997.6702>
- Wilhelmsson, U., Andersson, D., de Pablo, Y., Pekny, R., Stahlberg, A., Mulder, J., ... Pekna, M. (2017). Injury leads to the appearance of cells with characteristics of both microglia and astrocytes in mouse and human brain. *Cerebral Cortex*, 27(6), 3360–3377. <https://doi.org/10.1093/cercor/bhx069>
- Wilhelmsson, U., Li, L., Pekna, M., Berthold, C. H., Blom, S., Eliasson, C., ... Pekny, M. (2004). Absence of glial fibrillary acidic protein and vimentin prevents hypertrophy of astrocytic processes and improves post-traumatic regeneration. *The Journal of Neuroscience*, 24(21), 5016–5021. <https://doi.org/10.1523/JNEUROSCI.0820-04.2004>
- Winkler, J., Hagelstein, S., Rohde, M., & Laqua, H. (2002). Cellular and cytoskeletal dynamics within organ cultures of porcine neuroretina. *Experimental Eye Research*, 74(6), 777–788. <https://doi.org/10.1006/exer.2002.1188>
- Wu, K. H., Madigan, M. C., Billson, F. A., & Penfold, P. L. (2003). Differential expression of GFAP in early v late AMD: A quantitative analysis. *The British Journal of Ophthalmology*, 87(9), 1159–1166. <https://doi.org/10.1136/bjo.87.9.1159>

- Wunderlich, K. A., Tanimoto, N., Grosche, A., Zrenner, E., Pekny, M., Reichenbach, A., ... Perez, M. T. (2015). Retinal functional alterations in mice lacking intermediate filament proteins glial fibrillary acidic protein and vimentin. *The FASEB Journal*, 29(12), 4815–4828. <https://doi.org/10.1096/fj.15-272963>
- Young, R. W. (1985). Cell differentiation in the retina of the mouse. *The Anatomical Record*, 212(2), 199–205. <https://doi.org/10.1002/ar.1092120215>
- Zeisel, A., Hochgerner, H., Lönnerberg, P., Johnsson, A., Memic, F., van der Zwan, J., ... Linnarsson, S. (2018). Molecular architecture of the mouse nervous system. *Cell*, 174(4), 999–1014 e1022. <https://doi.org/10.1016/j.cell.2018.06.021>
- Zrenner, E., Bartz-Schmidt, K. U., Benav, H., Besch, D., Bruckmann, A., Gabel, V. P., ... Wilke, R. (2011). Subretinal electronic chips allow blind patients to read letters and combine them to words. *Proceedings of the Biological Sciences*, 278(1711), 1489–1497. <https://doi.org/10.1098/rspb.2010.1747>

## SUPPORTING INFORMATION

Additional supporting information may be found online in the Supporting Information section at the end of this article.

**How to cite this article:** Hippert, C., Graca, A. B., Basche, M., Kalargyrou, A. A., Georgiadis, A., Ribeiro, J., Matsuyama, A., Aghaizu, N., Bainbridge, J. W., Smith, A. J., Ali, R. R., & Pearson, R. A. (2021). RNAi-mediated suppression of vimentin or glial fibrillary acidic protein prevents the establishment of Müller glial cell hypertrophy in progressive retinal degeneration. *Glia*, 1–19. <https://doi.org/10.1002/glia.24034>